ACTA PHYSICA

ACADEMIAE SCIENTIARUM HUNGARICAE

ADIUVANTIBUS
R. GÁSPÁR, K. NAGY, L. PÁL, A SZALAY, I. TARJÁN

REDIGIT
I. KOVÁCS

TOMUS XLV

U. I. C. C.
APR 25 1980
LIBRARY

AKADÉMIAI KIADÓ, BUDAPEST
1978

Digitized by the Internet Archive
in 2024

https://archive.org/details/acta-physica-hungarica_1978_45_index

INDEX

Tomus 45

R. Cavalheiro and *M. M. Shukla:* Lattice Dynamics of Magnesium on Extended de Launay Model 3

A. Rai, M. Gaur and *R. Ram:* Propagation of Weak MHD Discontinuities in an Optically Thin Medium 9

A. Basu: Some Boundary Value Problems in Magneto-Elastodynamics 15

R. Gáspár and *R. Gáspár Jr.:* Bond Orbital Model of Molecules. The Model Potential Approach 27

N. M. Plakida and *T. Siklós:* Lattice Dynamics and Stability of Anharmonic Crystals ... 37

R. Cavalheiro and *M. M. Shukla:* Lattice Dynamics of Chromium on Extended de Launay Model 75

P. Singh and *D. K. Bhattacharya:* Application of G.P.D.P. to Thermal Boundary Layer 81

Д. Л. Беке, Ф. Ревес, Ф. Й. Кедвеш, Й. Гедень и *Й. Фелсерфалви:* О движении и кинетических формах пор в диффузионной зоне чистемы KCl—KBr 87

K. S. Shirkot and *S. Singh:* Unsteady Combined Free and Forced Convection Effects on the Flow in a Horizontal Channel 97

T. Singh and *R. B. S. Yadav:* Cylindrically Symmetric Self-Gravitating Fluids with Pressure Equal to Energy Density 107

R. Shankar and *S. K. Jain:* Formation of Shock Waves in Dissociating Gases 113

R. Gáspár and *I. Koós:* Calculations in a Model Potential Field for the Isoelectronic Scries of the Li Atom 123

R. Kępa: The Analysis of the Herzberg System in the $^{13}C^{16}O$ and Partly in the $^{12}C^{16}O$ Molecules 133

L. B. Rédei: Bound for the Harmonic Oscillator Greens Function 149

M. K. El-Mously, M. F. Kotkata and *S. A. Mazen:* Effect of Bi on the Annealing Kinetics of Amorphous As_2Se_3 153

L. M. Srivastava and *R. P. Agarwal:* On Unsteady Viscous MHD Flow through a Porous Channel with Constant Suction 163

T. M. Karade: On Stationary Spherically Symmetric Cluster of Particles 171

V. Vidyanidhi and *V. Dhananjaya Rao:* Heat Transfer through a Rotating Channel in Porous Medium 179

Y. Thomas et *P. Six:* Sur l'équivalence des théories de Grüneisen et de Brillouin pour la dilatation thermique des solides 191

P. Singh and *K. K. Srivastava:* Variational Solution of Heat Convection in the Channel Flow with the Help of GPDP 201

R. C. Sharma and *K. C. Sharma:* Rayleigh—Taylor Instability of Two Viscoelastic Superposed Fluids 213

C. Malinowska-Adamska: Potential Energy Parameters from Crystalline State Properties 221

M. Saleh and *M. S. Zafar:* Electron and Hole Generation in Anthracene under Electron Bombardment 233

M. F. Tolba, S. A. Wahab and *A. M. Salem:* On the Diurnal Variation Coefficients of the Nucleonic Component of Cosmic Rays 243

J. Giber, J. Kazsoki and *L. Koblinger:* Collision Cascades and the Disturbed Zone during Sputtering Processes (Model Computation) 275
RECENSIONES 279
Prof. Sándor Szalay 70 Years 283
P. P. Rao and *R. N. Tiwari:* A Class of Static Weyl Solutions for the Brans—Dicke Maxwell Fields 285
J. N. S. Kashyap: On Static Axially Symmetric Electrovac Universes 293
V. B. Johri, G. K. Goswami and *I. J. Singh:* Spatially Homogeneous and Anisotropic Expanding Universe 299
J. N. S. Kashyap: Coupled Electromagnetic and Scalar Fields in a Cylindrically Symmetric Space-Time 309
H. Farkas: Thermodynamic Concepts for a Class of One-Ports 317
I. Kovács, I. Péczeli and *A. Grandpierrè:* Contribution to the Intensity Distributions of the Multiplet Bands in Diatomic Molecules III 327
A. I. Kobylansky: The Effect of Rotation-Vibrational Interaction on the Line Intensities in the Optical Spectra of Diatomic Molecules 363
L. K. Patel: Einstein Universe with a Source-Free Electromagnetic Field 371
RECENSIONES 375

SCIENCE LIBRARY

ACTA PHYSICA

ACADEMIAE SCIENTIARUM HUNGARICAE

S 2

ADIUVANTIBUS

R. GÁSPÁR, K. NAGY, L. PÁL, A. SZALAY, I. TARJÁN

REDIGIT

I. KOVÁCS

TOMUS XLVI FASCICULUS 1

U. I. C. C.
NOV 1 1979
LIBRARY

AKADÉMIAI KIADÓ, BUDAPEST

1979

ACTA PHYS. HUNG. APAHAQ 46 (1) 1–54 (1979)

ACTA PHYSICA

ACADEMIAE SCIENTIARUM HUNGARICAE

SZERKESZTI

KOVÁCS ISTVÁN

Az *Acta Physica* angol, német, francia vagy orosz nyelven közöl értekezéseket. Évente két kötetben, kötetenként 4—4 füzetben jelenik meg. Kéziratok a szerkesztőség címére (1521 Budapest XI., Budafoki út 8.) küldendők.

Megrendelhető a belföld számára az Akadémiai Kiadónál (1363 Budapest Pf. 24. Bankszámla 215-11488), a külföld számára pedig a „Kultura" Külkereskedelmi Vállalatnál (1389 Budapest 62, P.O.B. 149. Bankszámla 217-10990), vagy annak külföldi képviseleteinél.

The *Acta Physica* publish papers on physics in English, German, French or Russian, in issues making up two volumes per year. Subscription: $ 36.00 per volume. Distributor: "Kultura" Foreign Trading Company (1389 Budapest 62, P.O. Box 149) or its representatives abroad.

Die *Acta Physica* veröffentlichen Abhandlungen aus dem Bereich der Physik in deutscher, englischer, französischer oder russischer Sprache, in Heften, die jährlich zwei Bände bilden.

Abonnementspreis pro Band: $ 36.00. Bestellbar bei »Kultura« Außenhandelsunternehmen (1389 Budapest 62, Postfach 149) oder seinen Auslandsvertretungen.

Les *Acta Physica* publient des travaux du domaine de la physique en français, anglais, allemand ou russe, en fascicules qui forment deux volumes par an.

Prix de l'abonnement: $ 36.00 par volume. On peut s'abonner à l'Entreprise du Commerce Extérieur «Kultura» (1389 Budapest 62, P.O.B. 149) ou chez représentants à l'étranger.

«*Acta Physica*» публикуют трактаты из области физических наук на русском, немецком, английском и французском языках.

«*Acta Physica*» выходят отдельными выпусками, составляющими два тома в год.

Подписная цена — $ 36.00 за том. Заказы принимает предприятие по внешней орговле «Kultura» (1389 Budapest 62, P.O.B. 149) или его заграничные представительства.

ACTA PHYSICA

ACADEMIAE SCIENTIARUM HUNGARICAE

ADIUVANTIBUS
R. GÁSPÁR, K. NAGY, L. PÁL, A. SZALAY, I. TARJÁN

REDIGIT
I. KOVÁCS

TOMUS XLVI FASCICULUS 1

AKADÉMIAI KIADÓ, BUDAPEST
1979

ACTA PHYS. HUNG.

INDEX

V. Siegel, L. Boros und *H.-H. Kirchner:* Über das TSEE-Adsorptionsmaximum Lithium-dotierter BeO-Keramiken 3

B. G. Verma and *J. P. Vishwakarma:* On a Plane Magnetogasdynamic Shock Wave of Variable Strength 13

M. F. Kotkata, M. K. El-Mously and *F. M. Ayad:* Light Effect on Amorphous Crystal Transition in $SSe_{22\cdot5}$ 19

K. N. Mehrotra and *J. P. Dixit:* Debye—Waller Factors of Platinum and Lead..... 27

M. L. Mittal and *D. Govinda Thirtha:* Non-Linear Hydromagnetic Waves in Two-Electron Temperature Plasma 31

G. Deb Ray: Similarity Solutions for Plane Relativistic Flow in a Homogeneous Medium 39

E. Lőrincz, P. Richter and *I. Péczeli:* Excitation Processes in a Hollow-Cathode He—Zn Discharge 45

RECENSIONES 53

Acta Physica Academiae Scientiarum Hungaricae, Tomus 46 (1), pp. 3—11 (1979)

ÜBER DAS TSEE-ADSORPTIONSMAXIMUM LITHIUM-DOTIERTER BeO-KERAMIKEN

Von

V. Siegel,[1] L. Boros[2] und H.-H. Kirchner[1]

[1] PHYSIKALISCH-TECHNISCHE BUNDESANSTALT BRAUNSCHWEIG, BRD

[2] RADIOLOGISCHE KLINIK DER SEMMELWEIS UNIVERSITÄT FÜR MEDIZINISCHE WISSENSCHAFTEN BUDAPEST, UNGARN

(Eingegangen: 3. XII. 1978)

Vergleichende Untersuchungen an undotierten und Li-dotierten BeO-Keramiken zeigen, dass in den letzteren das TSEE-Maximum bei etwa 275 °C irreversiblen Änderungen unterworfen ist. Während sich dieses Emissionsmaximum für die undotierten Proben nach einer speziellen Vorbehandlung und einem H-Ionenbeschuss nach anschliessender γ-Strahlenanregung beliebig oft aufbauen lässt, ist dies für die Li-dotierten Proben nur in den ersten Messzyklen der Fall, wenn die BeO-Probe bei 500 °C in feuchter Luft getempert und gelagert wird. Nach wiederholten thermischen Behandlungen an feuchter Luft und Auswertungen wird das adsorptionsinduzierte TSEE-Maximum auch nach einem intensiven H-Ionenbeschuss kaum sichtbar. Das heisst aber, dass die oberflächlichen Lithium-Atome ihre aktive Rolle als Adsorptionszentren verloren haben, sei es durch eine chemische Umwandlung oder durch den Verlust von Li-Atomen durch Abdampfen.

Einführung

Der Einsatz von BeO-Keramiken als Exoelektronen-Dosimeter hat gezeigt, dass die Exoelektronen-Ausbeute bei mehrfachen Bestrahlungen mit der gleichen Energiedosis von γ-Strahlen grossen Streuungen unterworfen ist [1]. Diese Streuungen können nicht mit der Auswertemethode erklärt werden, sondern sind mit den Adsorptionseigenschaften des BeO verbunden. So konnte in [2—7] gezeigt werden, dass adsorbierte Oberflächenschichten auf verschiedenen Oxiden die thermisch stimulierte Exoelektronenemission (TSEE) stark beeinflussen. Untersuchungen des Verhaltens der beiden TSEE-Maxima bei etwa 270 °C und 324 °C an BeO-Keramiken haben ergeben, dass insbesondere das Maximum bei 270 °C von adsorbierten OH-Gruppen und Wasserdampf beeinflusst wird [8].

Dotierung der BeO-Proben mit Lithium

Für die Dotierung der BeO-Keramiken mit einer Reinheit von 99,25% wurde in Vaseline dispergiertes metallisches Lithium verwendet, das möglichst gleichmässig und mit der gleichen Masse auf die Oberfläche der scheibenförmigen Proben aufgetragen wurde. Danach wurden die Proben 1 Stunde lang

bei 1000 °C in trockener Luft getempert und rasch abgekühlt. Wegen der grossen Streuung der Messwerte für die frisch dotierten BeO-Keramiken wurden sie anschliessend einer mehrmaligen Bestrahlung mit γ-Strahlen und Temperung bis 800 °C unterzogen [9]. Eine ähnliche Vorbehandlung der undotierten BeO-Proben stellte sicher, dass die Ergebnisse der weiteren Untersuchungen an beiden Probenarten verglichen werden konnten.

Vorbehandlung der Proben und Messmethode

Ausgehend von den durch Messungen der Infrarotspektren festgestellten Desorptionsprozesse auf keramischen BeO-Proben [10, 11] wurden sowohl die nicht dotierten [12] als auch die mit Li dotierten BeO-Keramiken einer speziellen Vorbehandlung unterzogen. Sie bestand darin, dass die scheibenförmigen Proben innerhalb des Zählers in einer trockenen Methan-Atmosphäre auf 400 °C aufgeheizt wurden, um den physikalisch adsorbierten Wasserdampf zu desorbieren. Nach einer Abkühlung auf 20 °C wurde die Probe innerhalb des Zählers einem Beschuss durch Wasserstoffionen unterworfen. Zu diesem Zweck wurde an den Zähldraht des Proportionalzählers eine so grosse positive Hochspannung angelegt, dass die Gasverstärkung in Methan einsetzen konnte, wenn die BeO-Probe von aussen mit γ-Strahlen eines radioaktiven Präparates bestrahlt wurde. In diesem Falle werden in den Metallwänden des Zählers Compton- und Photo-Elektronen erzeugt, die in der Methan-Atmosphäre positive Ionen infolge der Dissoziation des Methans und Elektronen erzeugen. Diese negative Ladungsträger gelangen in unmittelbarer Nähe des positiven Zähldrahts in eine kritische Feldstärke, in der sie durch Stossionisation Elektronenlawinen auslösen, die am Ausgang des Zählers als Impulse nachgewiesen werden.

Auf der anderen Seite entstehen durch die Dissoziation des Methans positive Ionen, von denen die leichtesten H^+ und H_2^+ unter anderem in Richtung zur Probe wandern und dort auf der Oberfläche teilweise adsorbiert werden können. Wenn man annimmt, dass die Gasverstärkung während der Ionen Bedeckung konstant ist, dann ist die Anzahl der gezählten Elektronenlawinen (Impulse) ein Mass für die Anzahl der adsorbierten H-Atome.

Diese Vorbehandlung der Proben und anschliessende Auswertung wurde in einem mit Methan gespülten fensterlosen Proportionalzähler [13] ausgeführt. Während der Messung der thermisch stimulierten Exoelektronenemission wurde die Probe linear mit einer Rate von etwa 1,4 $K \cdot s^{-1}$ aufgeheizt. Vor jeder Messung wurden die Proben im Zähler, um den Einfluss von Wasserdampf zu vermeiden, mit einer γ-Strahlenquelle (^{137}Cs oder ^{60}Co) angeregt.

Messergebnisse

a) *Undotierte BeO-Proben*

Ohne die oben beschriebene spezielle Vorbehandlung der undotierten BeO-Keramiken beobachtet man nach der Anregung mit γ-Strahlen nur das thermisch stimulierte Exoelektronen-Maximum bei etwa 325 °C (Bild 1a). Erst wenn der Wasserdampf desorbiert und H-Ionen adsorbiert wurden, erscheint nach der Anregung mit γ-Strahlen das neue TSEE-Maximum bei etwa 270 °C (Bild 1b) und c). Die Impulsanzahl N_{EE} dieses Maximums hängt von der Anzahl der registrierten Exoelektronenlawinen (Impulse) während des Ionenbeschusses bei eingeschalteter Hochspannung am Zähldraht ab. Wie man in Bild 2 erkennt, wird bereits bei etwa 3000 Impulsen eine Adsorp-

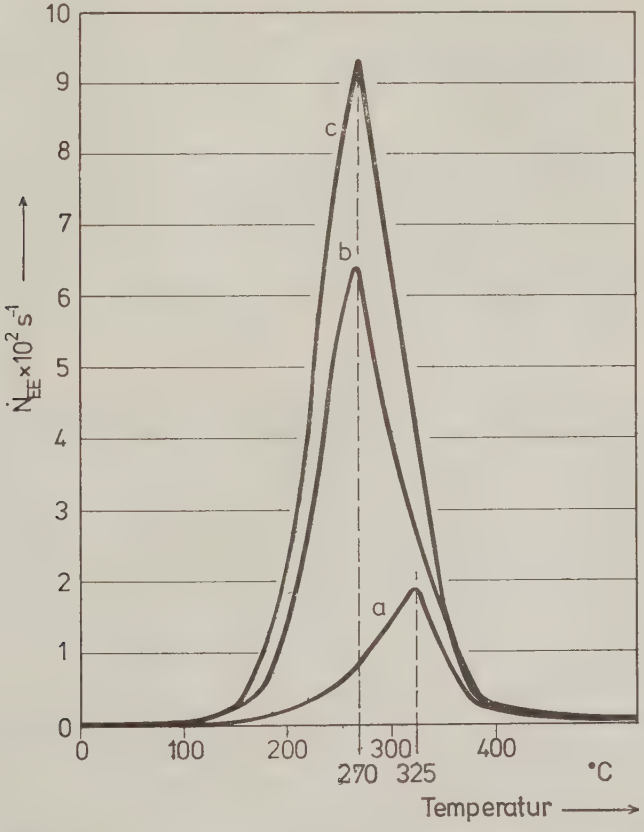

Bild 1. Änderung der TSEE-Maxima bei 270 °C und 325 °C in Abhängigkeit von der Vorbehandlung der undotierten BeO-Probe bei konstanter γ-Strahlenanregung. a — ohne Vorbehandlung, b — mit H-Ionenbeschuss (200 Impulse); c — (770 Impulse). $\dot{N}_{EE}$ — Impulsanzahl je Sekunde

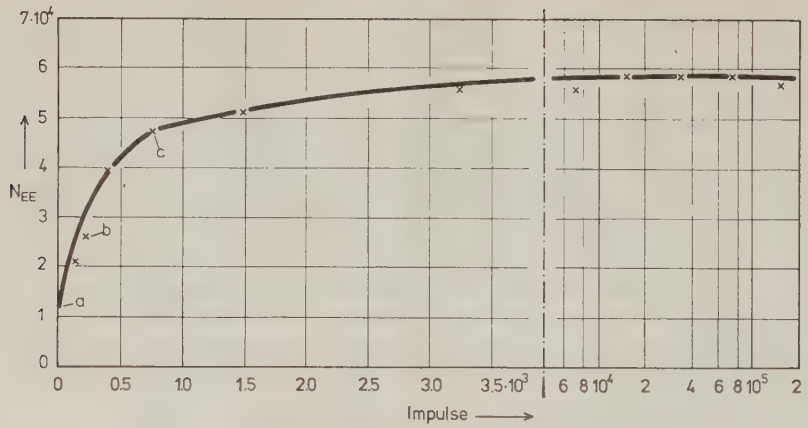

Bild 2. Änderung der Impulsanzahl N_{EE} für die undotierten BeO-Proben in Abhängigkeit von der Anzahl der erzeugten H-Ionen Impulse bei konstanter γ-Strahlenanregung. In Bild 1 sind die TSEE-Maxima für die Punkte a, b und c dargestellt

tionssättigung erreicht, da ein weiterer Ionenbeschuss keinen Anstieg der Exoelektronen-Ausbeute bei Anregung mit einer konstanten Energiedosis der γ-Strahlen zur Folge hat. Dieses neue TSEE-Maximum verschwindet wieder, wenn die speziell vorbehandelte BeO-Probe vor der γ-Strahlen-Anregung an feuchte Luft gebracht wird [9, 12].

b) *Li-dotierte BeO-Proben*

Dieselben Behandlungsmethoden und Messungen wie an den undotierten BeO-Keramiken wurden auch an den mit Lithium dotierten ausgeführt. Auch hier zeigen die nicht speziell vorbehandelten Proben nur das TSEE-Maximum bei 325 °C (Bild 3a). Auffällig ist hier aber, dass die Exoelektronen-Ausbeute N_{EE} bei gleicher Energiedosis der γ-Strahlen um den Faktor 10 bis 15 grösser ist als bei den undotierten BeO-Proben, d.h. die Li-dotierten BeO-Keramiken sind sehr viel empfindlicher [14]. Nach dem Ionenbeschuss innerhalb der Methan-Atmosphäre des Zählers erscheint wie im Falle der undotierten BeO-Keramiken nach der γ-Strahlen-Angerung das neue TSEE-Maximum bei etwa 275 °C (Bild 3b—d). Im Gegensatz zu den undotierten Proben liegt die Adsorptionssättigung für die Li-dotierten Proben bei der doppelten Anzahl von registrierten Elektronenlawinen (etwa 6000) während des Ionenbeschusses. Bei gleicher Energiedosis der anschliessenden γ-Bestrahlung liegt die Exoelektronen-Ausbeute im Bereich der Sättigung für die undotierte Probe bei $N_{EE} = 5{,}8 \cdot 10^4$, für die Li-dotierte BeO-Probe bei $N_{EE} = 8{,}6 \cdot 10^5$. Offenbar ist die Anzahl der besetzbaren Adsorptionsplätze auf Grund der Dotierung mit Lithium stark angestiegen.

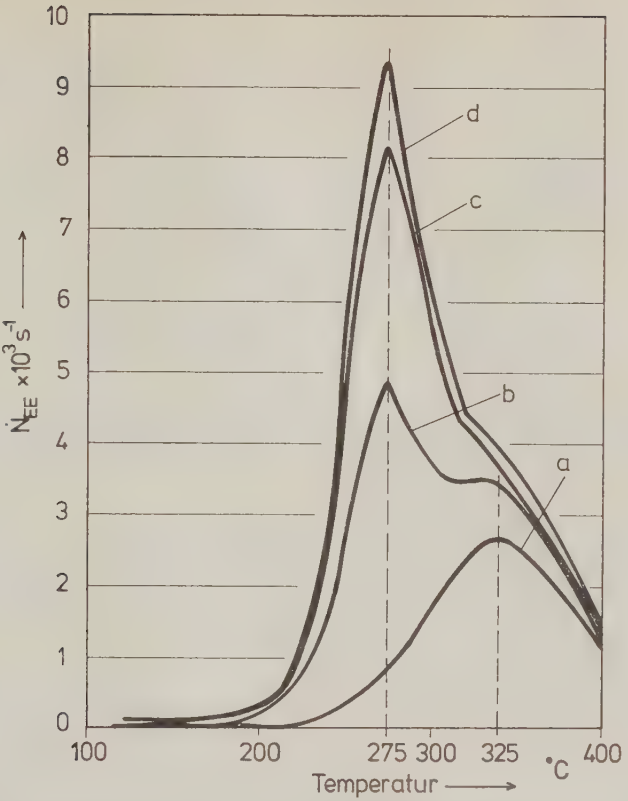

Bild 3. Änderung der TSEE-Maxima bei 275 °C und 325 °C in Abhängigkeit von der Vorbehandlung der Li-dotierten BeO-Proben bei konstanter γ-Strahlenanregung. a – ohne Vorbehandlung, b bis d mit H-Ionenbeschuss (b — 500, c — 1000, d — 5000 Impulse)

Wie im Falle der undotierten BeO-Proben wurden auch die dotierten vor jeder Messung bei 500 °C an feuchter Luft getempert, abgekühlt und gelagert. Dabei zeigte sich nach mehrfacher Verwendung derselben Proben ein neuer Effekt. Nach der eingangs beschriebenen speziellen Vorbehandlung und anschliessenden γ-Strahlenanregung sollte man wieder das neue TSEE-Maximum bei 275 °C erwarten. Wie Bild 4 aber zeigt, erscheint es bei einer registrierten Anzahl von 1000 Elektronenlawinen überhaupt nicht (Bild 4a) im Gegensatz zu Bild 3c, wo ebenfalls 1000 Elektronenlawinen an der frischen Probe gezählt wurden. Nach diesem Messzyklus wurde dieselbe BeO-Probe vor der speziellen Vorbehandlung mehrere Male bei 500 °C an Luft getempert. Die anschliessenden Messungen, ausgeführt wie zuvor, ergaben erneut, dass sich das TSEE-Maximum bei 275 °C nicht mehr aufbauen liess. Erst bei einer Anzahl registrierter Elektronenlawinen von 8000 (Kurve b) und 17 000

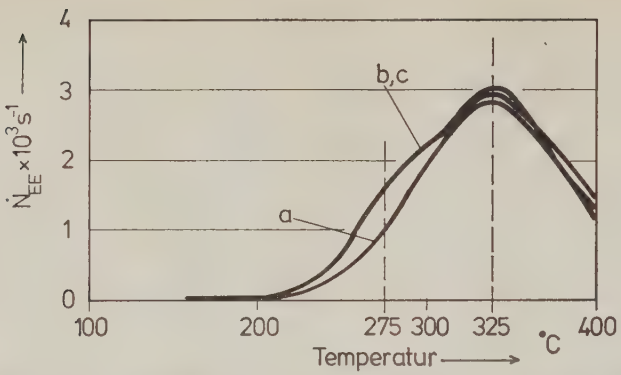

Bild 4. Änderung der TSEE-Maxima bei 275 °C und 325 °C in Abhängigkeit von der Vorbehandlung für eine mehrfach getemperte Li-dotierte BeO-Probe bei konstanter γ-Strahlenanregung. a bis c mit H-Ionenbeschuss (a — 3000, b — 8000, c — 17 000 Impulse)

(Kurve c) zeigt sich eine Andeutung des Maximums bei 275 °C. Nur an einer frischen Li-dotierten BeO-Keramik-Probe beobachtet man den wachsenden Anstieg des TSEE-Maximums bei 275 °C mit ansteigender Anzahl der registrierten Elektronenlawinen, wie er in Bild 3 dargestellt ist.

Dieses abweichende Verhalten der Li-dotierten BeO-Proben gegenüber dem H-Ionenbeschuss legt die Vermutung nahe, dass sich das Lithium auf der BeO-Oberfläche chemisch verändert hat oder abgedampft ist. Für einen Verlust an Lithium spricht eine Massenbestimmung des Li an einer unbehandelten und der hier mehrfach verwendeten BeO-Probe. Die unbehandelte Probe enthielt 210 μg Li, die mehrfach verwendete dagegen nur 60 μg Li. Diese Schlussfolgerung gilt aber nur für den Fall, dass beide Proben im Anfangszustand die gleiche Masse an Lithium enthielten, was nicht mehr kontrollierbar ist.

Aus [15] ist bekannt, dass sich bei der Einwirkung von H^+-Ionen oder H_2-Molekülen auf das Li schon bei 20 °C die sehr beständige Verbindung LiH bildet. Dieses LiH wird aber bei höheren Temperaturen durch das Einwirken des Luft-Stickstoffes im Beisein von Wasserdampf zum grösseren Teil in die Verbindung $LiNH_2$, Li_2NH und Li_3N und zum kleineren Teil in Li_2O umgewandelt.

Die oben beschriebenen Messungen an den Li-dotierten BeO-Keramiken wurden in Unkenntnis der eben genannten chemischen Umwandlungen nach dem Tempern und Lagern der Proben an feuchter Luft ausgeführt.

Im folgenden wurden die BeO-Keramiken um diese chemischen Umwandlungen zu vermeiden, vor jeder Messung

a) bei 1000 °C in trockener Luft oder Argon getempert und abgekühlt und anschliessend in einer trockenen Atmosphäre im Exsikkator gelagert,

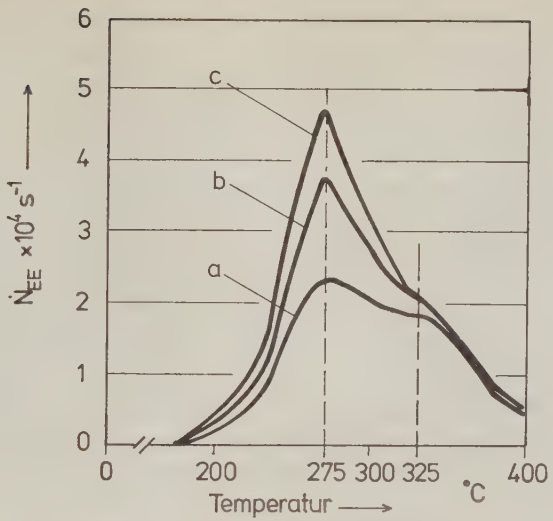

Bild 5. Änderung der TSEE-Maxima bei 275 °C und 325 °C einer Li-dotierten BeO-Probe nach dem Tempern und Lagern in trockener Luft und anschliessender konstanter γ-Strahlenanregung. H-Ionenbeschuss, a — 500, b — 1000, c — 5000 Impulse

b) bei 1000 °C in Argon getempert und anschliessend in feuchter Luft abgekühlt und gelagert.

Die Ergebnisse der Messreihe a) zeigen an einem Beispiel Bild 5 und der Messreihe b) Bild 6.

Nach dem Tempern in trockener Luft und der Lagerung im Exsikkator bleibt das TSEE-Adsorptionsmaximum bei 275 °C nach der gleichen Anzahl von gezählten Elektronenlawinen (Impulsen) und nach der Anregung mit der gleichen Energiedosis der γ-Quanten auch nach der 12. Messung über einen Zeitraum von 3 Wochen praktisch konstant. Wie Bild 5a—c zeigt, hängt die Impulsanzahl N_{EE} des TSEE-Maximums bei 275 °C wie bei einer frischen Probe von der Anzahl der gezählten Impulse beim Ionenbeschuss ab. Da das TSEE-Maximum bei 325 °C unbeeinflusst bleibt, bedeutet dies, dass die Empfindlichkeit der BeO-Probe über längere Zeit konstant bleibt.

Anders verhält es sich mit den Proben, die in Argon getempert und anschliessend an feuchter Luft gelagert wurden. Wie die Bilder 6 A und B zeigen, lässt sich zwar durch den H^+-Ionenbeschuss das TSEE-Maximum bei 275 °C erzeugen, aber die Impulsanzahl N_{EE} fällt von 100% bei der 1. bis 4. Messung (Bild 6 A) auf 50% bei der 18. Messung (Bild 6 B) ab. Dagegen sinkt die Impulsanzahl N_{EE} für das TSEE-Maximum bei 325 °C in derselben Messreihe nur um 25% vom ursprünglichen Wert ab. Beim Tempern der Proben bei 1000 °C in trockener Luft oder Argon werden die Lithiumnitride offenbar wieder reduziert, bilden sich aber erneut langsam beim Abkühlen und Lagern in feuchter Luft. Wie die Messreihe b) zeigt, überwiegt

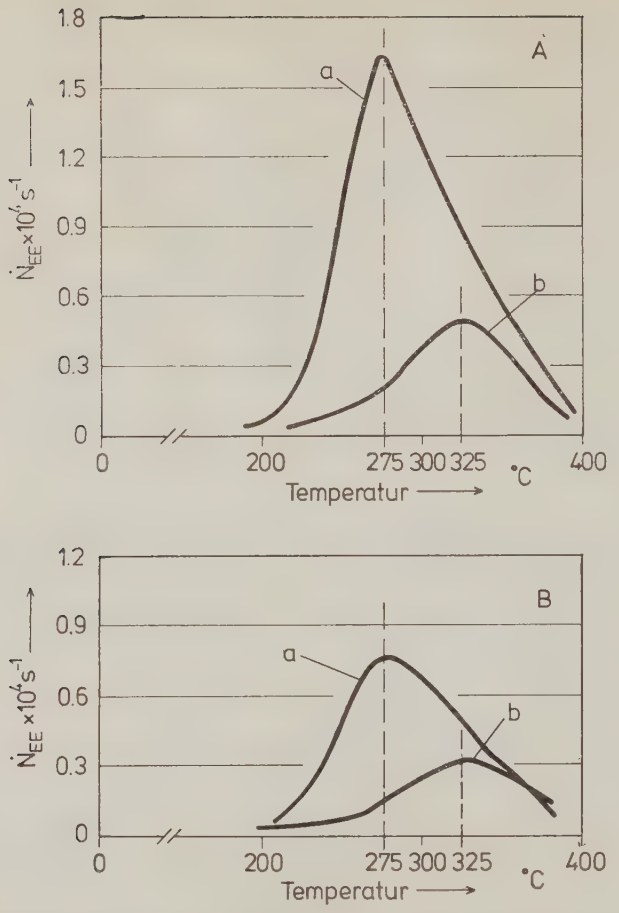

Bild 6. Änderung der TSEE-Maxima bei 275 °C und 325 °C einer Li-dotierten BeO-Probe nach Tempern in Argon und Lagern in feuchter Luft. a — Ionenbeschuss etwa 5000 Impulse, b — ohne H-Ionenbeschuss. A — 4. Messung; B — 18. Messung

jedoch die Bildung der Nitride, da die Impulsanzahl N_{EE} des TSEE-Adsorptionsmaximums unter gleichen Vorbehandlungs- und Anregungsbedingungen im Verlauf der Messreihe stetig abnimmt.

Diskussion

In [14] wurde gezeigt, dass die Empfindlichkeit der Li-dotierten BeO-Keramiken konstant bleibt bei einer Lagerung in einer Argon-Atmosphäre, während die Reproduzierbarkeit der Messwerte in anderen Gasen (Sauerstoff,

Stickstoff, Luft) schlechter war. Betrachtet man das Verhalten der beiden TSEE-Maxima in feuchter Luft, so ändert sich bei gleichen Anregungsbedingungen insbesondere das adsorptionsinduzierte TSEE-Maximum bei 275 °C. Für das Lithium ist bekannt, dass es im adsorbierten Zustand als Donator-Zentrum wirkt, auch wenn es als Li_2O oder LiOH auf der Oberfläche eines Oxids vorliegt [18]. Beide Verbindungen reagieren aber bei höheren Temperaturen, ebenso wie LiH, im Beisein von Wasserdampf mit dem Luft-Stickstoff unter Bildung von $LiNH_2$, Li_2NH und Li_3N. Von diesen Verbindungen weiss man, dass sie in adsorbierter Form als Akzeptor Zentren wirken.

Offenbar wird durch diese Verbindungen beim Ionenbeschuss die Adsorption von H^+ und H_2^+ verhindert, die auf dem BeO OH-Gruppen bilden, welche bei der assoziativen Desorption Elektronen freisetzen, die als Exoelektronen nachgewiesen werden [9, 12]. Die drei Verbindungen Li_2NH, $LiNH_2$ und Li_3N zeigen denselben Vergiftungseffekt für die aktiven Oberflächenzentren der Exoelektronenemission wie adsorbierte Alkohole [16, 17], mit dem Unterschied, dass sie selektiv nur die Adsorptionsplätze für das TSEE-Maximum bei 275 °C blockieren.

Wenn man die hohe Empfindlichkeit der Li-dotierten BeO-Keramiken gegenüber ionisierenden Strahlen konstant halten will, muss man den Einfluss feuchter Luft vermeiden, um die sensibilisierende Wirkung des Lithiums auf der BeO-Oberfläche nicht durch chemische Umwandlungen zu gefährden.

LITERATUR

1. V. Siegel and W. Rasp, Actes du VIII^e Congrès International de la Société Francaise de Radioprotection, Saclay, 1977, p. 380.
2. I. V. Krylova, phys. stat. solidi (a), **7**, 359, 1971.
3. N. I. Konyushkina und I. V. Krylova, Fiz. Tverd. Tela, **15**, 1925, 1973.
4. I. V. Krylova, Proc. 4th Intern. Symp. on Exoelectron Emission and Dosimetry, Liblice/CSSR, 1973, p. 145.
5. M. Euler, W. Kriegseis und A. Scharmann, phys. stat. solidi (a), **15**, 431, 1973.
6. W. Kriegseis und A. Scharmann, phys. stat. solidi (a), **29**, 407, 1975.
7. M. Euler und A. Scharmann, phys. stat. solidi (a), **34**, 297, 1976.
8. V. Siegel, W. Rasp und H.-H. Kirchner, phys. stat. solidi (a), **42**, K 147, 1977.
9. L. Boros, Acta Phys. Hung., **34**, 255, 1973.
0. S. E. Ermatov und T. S. Kosherov, Izv. Akad. Nauk Kazak SSR, Ser. Fiz.-Mat., **12**, 29, 34, 1974.
1. S. E. Ermatov, Zh. Prikl. Spektrosk., **23**, 14, 1975.
2. V. Siegel, W. Rasp und H.-H. Kirchner, wird veröffentlicht.
3. H.-J. Kriks und W. Schaare, PTB-Mitt., **81**, 10, 1971.
4. D. F. Regulla, G. Drexler und L. Boros, Proc. Third Intern. Conf. on Luminescence Dosimetry, Riso/Denmark, Rep. No. 249, 1971, p. 601.
5. Gmelins Handbuch der anorganischen Chemie, Ser.-Nr. 20, Li, 8. Auflage, 1960, Verlag Chemie GmbH Weinheim/Bergstr.
6. V. Siegel, W. Rasp und H.-H. Kirchner, phys. stat. solidi (a), **34**, K 203, 1976.
7. V. Siegel, W. Rasp und H.-H. Kirchner, Proc. 5th Intern. Symp. on Exoelectron Emission and Dosimetry. Zvikov/CSSR, 1976, p. 58.
8. D. G. Thomas, J. Phys. Chem. Solids, **9**, 31, 1958.

Acta Physica Academiae Scientiarum Hungaricae, Tomus 46 (1), pp. 13—18 (1979)

ON A PLANE MAGNETOGASDYNAMIC SHOCK WAVE OF VARIABLE STRENGTH

By

B. G. Verma and J. P. Vishwakarma

DEPARTMENT OF MATHEMATICS, UNIVERSITY OF GORAKHPUR, GORAKHPUR 273001, U. P., INDIA

(Received 5. XII. 1978)

A particular solution of the equations of one dimensional anisentropic flow of a polytropic gas is linked by a magnetogasdynamic shock to gas at rest in which the density is non-uniform and magnetic field is constant. The approach is inverse in the sense that the density distribution is derived from the position of the shock and the prescribed flow behind it. The velocity and strength of the shock each vary with time.

1. Introduction

Copson [1], Mackie and Weir [2] and many other authors have discussed the problem of shock waves of constant strength moving with variable velocity. In these problems, there occurs a jump in the entropy across the shock, but the entropy remains uniform (at different levels) on both sides of the shock. More general situations are that in which a shock leaves a non-uniform distribution of entropy behind. Smith [3] has discussed a problem of such a flow in ordinary gasdynamics. The present paper extends the discussion of Smith's problem to a perfectly conducting gas in the presence of a transverse magnetic field. We have started from a known anisentropic flow and linked it through a shock wave to gas at rest. The state of the stationary gas is not known until the shock path has been determined. It is shown that the velocity and strength of the shock each vary with time.

For the anisentropic flow behind the shock, we have used the family of exact solutions obtained by Weir [4].

2. Weir's solution

With viscosity and heat conduction neglected, the relevant equations for one-dimensional anisentropic flow are,

$$\frac{\partial \varrho}{\partial t} + u\frac{\partial \varrho}{\partial x} + \varrho\frac{\partial u}{\partial x} = 0, \tag{2.1}$$

$$\frac{\partial u}{\partial t} + u\frac{\partial u}{\partial x} + \frac{1}{\varrho}\frac{\partial p}{\partial x} + \frac{\mu h}{\varrho}\frac{\partial h}{\partial x} = 0, \tag{2.2}$$

$$\frac{\partial S}{\partial t} + u\frac{\partial S}{\partial x} = 0, \tag{2.3}$$

where p, ϱ, h, S, u and μ are respectively pressure, density, magnetic field, specific entropy, fluid velocity and magnetic permeability. For a polytropic gas the equation of state is

$$p = K\varrho^{\gamma} \exp\left(\frac{S}{C_v}\right), \tag{2.4}$$

where γ is the constant adiabatic index, C_v the specific heat at constant volume and K is the dimensional constant.

It can be verified that Eqs. (2.1) to (2.4) possess a solution (c.f. WEIR's solution [4])

$$u_{02} = 2\alpha t + \delta, \tag{2.5}$$

$$p^*_{02} = f(X), \tag{2.6}$$

$$\varrho_{02} = \frac{1}{2\alpha}\frac{df}{dX}, \tag{2.7}$$

where

$$p^*_{02} = p_{02} + \frac{1}{2}\mu h^2_{02}, \; p_{02} = \beta p^*_{02}, \; (0 < \beta < 1)$$

and particle paths are given by

$$X = x - \alpha t^2 - \delta t, \tag{2.8}$$

X being the material variable and the suffix 02 is introduced to distinguish between the WEIR's solution and the state of the gas behind the shock. The pressure and density are constant along the particle paths which are coaxial parabolas in the (x, t) — plane.

3. The shock path

We shall now link the solution given in Section 2 to a state of rest through magnetogasdynamic shock relations for a polytropic gas, namely:

$$\varrho_2 v_2 = \varrho_1 v_1, \tag{3.1}$$

$$h_2 v_2 = h_1 v_1, \tag{3.2}$$

$$p_2 + \frac{1}{2}\mu h_2^2 + \varrho_2 v_2^2 = p_1 + \frac{1}{2}\mu h_1^2 + \varrho_1 v_1^2, \tag{3.3}$$

$$\frac{\gamma}{\gamma - 1}\frac{p_2}{\varrho_2} + \frac{\mu h_2^2}{\varrho_2} + \frac{1}{2}v_2^2 = \frac{\gamma}{\gamma - 1}\frac{p_1}{\varrho_1} + \frac{\mu h_1^2}{\varrho_1} + \frac{1}{2}v_1^2, \tag{3.4}$$

where v is the velocity of the gas relative to the velocity of the shock and suffixes 2 and 1 are attached to the states immediately behind and in front (the stationary gas) of the shock, respectively.

These shock relations must be satisfied at the shock whose displacement is taken as $\xi = \xi(t')$, where the prime has been added to the time t since we shall subsequently use it as a parameter. From (2.8)

$$X = \xi(t') - \alpha t'^2 - \delta t' \tag{3.5}$$

on the shock. It then follows from (2.5), (2.6) and (2.7) that

$$u_2 = 2\alpha t' + \delta, \tag{3.6}$$

$$p_2^* = g(t'), \tag{3.7}$$

$$\varrho_2 = -\frac{\dot{g}(t')}{2\alpha[\dot{\xi}(t') - 2\alpha t' - \delta]}, \tag{3.8}$$

where

$$g(t') = f\{\xi(t') - \alpha t'^2 - \delta t'\}$$

and

$$p_2 = \beta p_2^*, \quad p_2^* = p_2 + \frac{1}{2}\mu h_2^2, \quad (0 < \beta < 1).$$

Furthermore,

$$v_2 = 2\alpha t' + \delta - \xi(t').$$

In front of the shock, we take the gas to be at rest so that $u_1 = 0$ and $v_1 = -\dot{\xi}(t')$. Further, $p_1^* = p_1 + \mu h_1^2/2 = k$, a constant, since h_1 is taken to be constant and by equation (2.2) the pressure gradient must be zero.

The elimination of the unknown ϱ_1 between equations (3.1) and (3.3) yields

$$p_2^* - p_1^* = \varrho_2 v_2 (v_1 - v_2). \tag{3.9}$$

Similarly from Eqs. (3.1), (3.2) and (3.4) we get

$$\left[v_1\left\{\frac{\gamma\beta}{\gamma - 1} - 2(1 - \beta)\right\} - v_2\frac{(\gamma - 2)(1 - \beta)}{(\gamma - 1)}\right]p_2^* v_2 - \frac{\gamma}{\gamma - 1}p_1^* v_1^2$$

$$= \frac{1}{2}\varrho_2 v_2 v_1 (v_1^2 - v_2^2). \tag{3.10}$$

Direct substitution in (3.9) and (3.10) of the flow quantities given previously yields

$$(2\alpha t' + \delta)\dot{g} + 2\alpha g - 2\alpha k = 0, \tag{3.11}$$

$$2\alpha\gamma(g - k)\dot{\xi}^2 - (\gamma - 1)(2\alpha t' + \delta)[(2\alpha t' + \delta)/2 - \dot{\xi}]\dot{g}\dot{\xi}$$
$$- 2\alpha(2\alpha t' + \delta)[\gamma^*\dot{\xi} + (\gamma - 2)(1 - \beta)(2\alpha t' + \delta)]g = 0, \tag{3.12}$$

where

$$\gamma^* = \gamma\beta + 2(1 - \beta).$$

Solving the differential equation (3.11), we have

$$g = \frac{2\alpha k t' + A}{2\alpha t' + \delta}, \quad t' \neq -\delta/2\alpha, \tag{3.13}$$

where A is a constant. The elimination of g between (3.12) and (3.13) yields the shock velocity as

$$\dot{\xi} = \frac{1}{2}(2\alpha t' + \delta)\left\{b + \left[b^2 + 4(\gamma - 2)(1 - \beta)\left(\frac{2\alpha t' + \delta}{\gamma} B + 1\right)\right]^{\frac{1}{2}}\right\}, \tag{3.14}$$

where

$$b = (2\alpha t' + \delta)\frac{B\gamma^*}{\gamma} + \left(\gamma^* - \frac{\gamma - 1}{2}\right),$$

and

$$B = \frac{k\gamma}{A - k\delta}.$$

Integrating the Eq. (3.14), we get the shock path as

$$\xi = \frac{\gamma^* B}{12\gamma\alpha}(2\alpha t' + \delta)^3 + \frac{1}{8\alpha}\left(\gamma^* - \frac{\gamma - 1}{2}\right)(2\alpha t' + \delta)^2 + C$$
$$+ \frac{1}{12N}(2\alpha t' + \delta)^2\left[b^2 + 4(\gamma - 2)(1 - \beta)\left(\frac{2\alpha t' + \delta}{\gamma} B + 1\right)\right], \tag{3.15}$$

where

$$N = b\left[\frac{2\alpha\gamma^* B}{\gamma}(2\alpha t' + \delta) + \alpha\left(\gamma^* - \frac{\gamma - 1}{2}\right)\right] +$$
$$+ 2\alpha(\gamma - 2)(1 - \beta)\left[\frac{3B}{\gamma}(2\alpha t' + \delta) + 2\right]$$

and C is a constant. Thus the shock relations determine the shock path and fix the flow quantities on both sides of the shock. In terms of the spatial variables, the total pressure and density behind the shock are given parametrically by

$$p_2^* = \frac{2\alpha k t' + A}{2\alpha t' + \delta}, \tag{3.16}$$

$$\varrho_2 = \frac{2(A - k\delta)}{(2\alpha t' + \delta)^3 (b - 2 + L)}, \tag{3.17}$$

$$x - \alpha t^2 - \delta t = \xi(t') - \alpha t'^2 - \delta t', \tag{3.18}$$

where

$$L = \left[b^2 + 4(\gamma - 2)(1 - \beta) \left(\frac{2\alpha t' + \delta}{\gamma} B + 1 \right) \right]^{\frac{1}{2}}.$$

The Eqs (3.16) and (3.17) follow from (3.7) and (3.8), and (3.18) is obtained by eliminating X between (2.8) and (3.5).

For the stationary gas in front of the shock, the density is given parametrically by

$$\varrho_1 = \frac{2(A - k\delta)}{(2\alpha t' + \delta)^3 (b + L)}, \tag{3.19}$$

$$x = \xi(t'). \tag{3.20}$$

Eq. (3.19), the density distribution as a function of time of the shock path, is obtained by calculating ϱ_1 from (3.1). To obtain the density as a function of x, we eliminate t' between (3.19) and the Eq. (3.20) of the shock path. Finally, the entropy of the stationary gas can then be derived from the equation of state (2.4) as a function of x.

4. Results and discussion

We have found a family of solutions whose members depend on the choice of values for the various constants. We assume $\alpha > 0$, $\delta > 0$ and $t \geq 0$. The shock must be compressive, that is, $0 < p_1^* < p_2^*$, or $0 < k < (2\alpha k t' + A)/(2\alpha t' + \delta)$. Thus $A - k\delta > 0$ and all pressures are positive. Inspection of (3.17) and (3.19) indicates that densities are positive if $\gamma > 1$.

Taking $\sigma = p_2/p_1$ as a measure of strength of the shock wave, we have maximum value of σ at $t = 0$ and $\sigma \to 1$ as $t' \to \infty$. Hence the strength of shock wave decreases with time. Also from (3.14), the shock velocity $\dot{\xi} \to \infty$ as $t' \to \infty$.

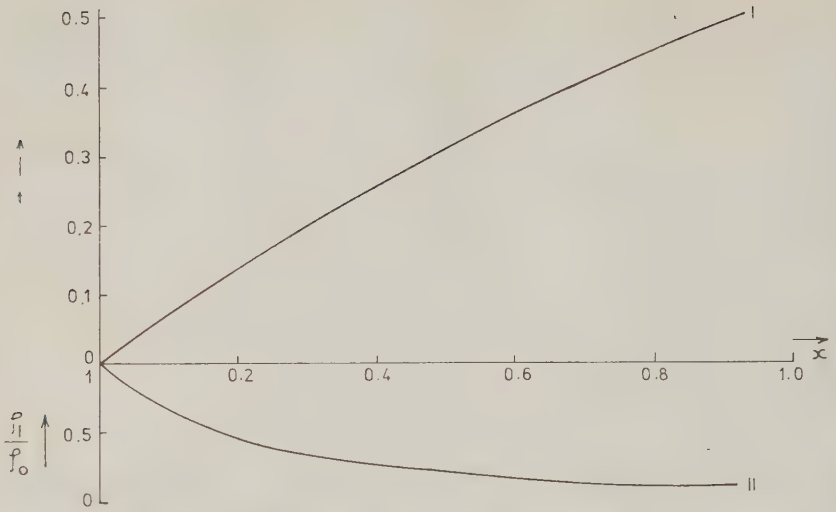

Fig. 1. Shock path in (x, y) plane (I). Variation of density with distance in the gas ahead of the shock (II)

Fig. 1. shows a typical configuration of the shock path in the (x, t) plane. The lower part of the Figure gives the density ratio in the gas upstream of the shock; ϱ_0 is the density at $x = 0$, $t = 0$. The value chosen for the various constants are as follows:

$$\alpha = \delta = 1;\ B = \frac{1}{2}(\gamma - 1);\ C = -\frac{5\gamma + 4}{40};\ \beta = \frac{2}{5};\ \gamma = \frac{7}{5}.$$

If $\alpha > 0$, the particle trajectories behind the shock are a family of straight lines with fluid velocity $u = \delta$. The gas ahead of the shock is at rest with constant density. The shock velocity is also constant and is given by

$$\dot{\xi} = \frac{\delta}{2}\left\{B\frac{\delta\gamma^*}{\gamma} + \left(\gamma^* - \frac{\gamma - 1}{2}\right) + \left[\left(\frac{B\delta\gamma^*}{\gamma} + \gamma^* - \frac{\gamma - 1}{2}\right)^2 + \right.\right.$$
$$\left.\left. + 4(\gamma - 2)(1 - \beta)\left(\frac{\delta B}{\gamma} + 1\right)\right]^{\frac{1}{2}}\right\}.$$

REFERENCES

1. E. T. Copson, Proc. Roy. Soc., A **222**, 254, 1954.
2. A. G. Mackie and D. G. Weir, Proc. Camb. Phil. Soc., **56**, 64, 1960.
3. P. Smith, Proc. Edinburgh Math. Soc., **13**, 297, 1963.
4. D. G. Weir, Proc. Camb. Phil. Soc., **57**, 890, 1961.

Acta Physica Academiae Scientiarum Hungaricae, Tomus 46 (1), pp. 19—26 (1979)

LIGTH EFFECT ON AMORPHOUS CRYSTAL TRANSITION IN $SSe_{22.5}$

By

M. F. Kotkata, M. K. El-Mously and F. M. Ayad

PHYSICS DEPARTMENT, FACULTY OF SCIENCE, AIN-SHAMS UNIVERSITY, CAIRO, EGYPT

(Received in revised form 10. XII. 1978)

Isothermal phase transformation of massive $SSe_{22.5}$ in the presence and absence of light illumination has been carried out in the temperature range of 98—144 °C using the electric conductivity method. Illumination affects the nucleation process through "photo-nucleation". Kinetic studies have not, to date, been presented so as to identify separately the light effects on the crystallization processes of materials of Se-like structure. The obtained conductivity data are presented as power and logarithmic functions to study the crystallization kinetics in the light of the present concepts of crystallization in organic polymers.

Introduction

Studies of the morphology of crystalline selenium indicate that it crystallizes from the bulk amorphous phase by chain folding [1—3]. Selenium forms extended-chain crystals by a thickening mechanism similar to that found in organic polymers [3]. Spherulites in bulk polymers grow outward from a nucleation centre that is frequently of a heterogeneous character. The radial growth of a spherulite is commonly the result of the formation of stacks of bladelike lamellas that grow outward from the nucleation centre. In addition, the crystallization of amorphous selenium involves both the crystallization of polymeric Se_n chains and the polymerization of Se_8 rings [4].

The addition of an isoelectronic element as sulphur does not cause a great disturbance in the short-range order of the atomic distribution of selenium [5]. But, 3—5 at % sulphur doped in selenium results in minimizing the rate of crystallization [6, 7]. Light, on the other hand, can produce a marked enhancement on the crystallization kinetics over that obtained from purely thermal effects [8—11]. This effect has been used to write holograms [12] and discrete images [10] with lasers.

In this paper, quantitative data on percent crystallization in the absence and presence of photo illumination for S-doped Se amorphous sample, namely $SSe_{22.5}$, are estimated from recording the electric conductivity changes continuously during isothermal transformation processes. A kinetic study is presented using Avrami's theory.

Experimental

Bulk $SSe_{22.5}$ samples have been prepared in the amorphous phase through heating the constituents at 280 °C for 2 hrs and quenching in air at 18—20 °C inside evacuated [10^{-4} mm Hg] pyrex cells having parallel faces (~2 mm apart) and provided with two tungsten electrodes.

Crystallization has been carried out in preheated ovens (0.2 °C max. fluctuations) under dark and illuminated conditions. Illumination was achieved by a 250 W ultra high pressure Hg-quartz lamp. The IR part of the emitted spectrum was filtered out to reduce sample heating.

The crystallization was monitored by measuring the electronic conduction periodically (1/2 min interval) during several isothermal transformations in the range 98—144 °C using an electrometer with an error less than 2%. The remarkable increase of the electric conductivity accompanying the amorphous to crystalline phase change (in the absence or presence of light) implies that the measured conductivity σ at any time t is the result of two conductivities σ_a and σ_c corresponding to a double phase system, amorphous and crystalline.

Results and discussion

The use of conductivity-structure characterization for a proper description of the volume fraction which has crystallized depends on the specific regimes of percent transformation. Therefore, the time-dependence of the electronic conduction of $SSe_{22.5}$ is represented as power and logarithmic dependence and is given in Fig. 1 for some isotherms.

During the transformation process, whether purely thermal or with the photon effect, there appear to be at least three regimes of σ versus percent transformation: The conductivity remains at first approximately constant, but after a certain time depending on annealing temperatures it increases abruptly by several orders to attain a certain maximum value. Such a strong increase of σ is due mainly to the transformation of the very low conductivity amorphous into a continuous path of rather better conducting crystalline $SSe_{22.5}$. The constancy of the maximum conductivity attained at a given temperature indicates the stability of the transformed products. Such maximum value varies with temperature and so it may not always correspond to the same degree of structural perfection but may rather refer to the degree of crystallization [13].

In Fig. 1, the minimum to apparent maximum of log σ proceeds in a smooth stage *ad* for the non-illuminated and in two distinguishable stages *ab* and *cd* for illuminated samples. The decrease in log σ in the period *bc* is ascribed to photo effects. Such effects are more pronounced in the range 108

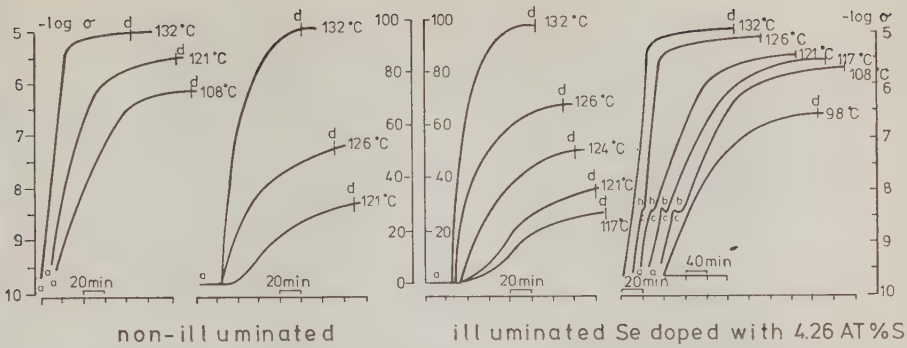

Fig. 1. Time-dependence of the electronic conduction represented as σ and log σ for Se doped with 4.26 at % S annealed under: (a) dark and (b) photo illumination for a variety of isotherms

to 126 °C when the isothermal time-dependence of the electronic conduction is represented as log σ_t rather than σ_t. Table I summarizes the effect of temperature on time and log σ associated with the individual stages together with the total change of log σ due to the crystallization of $SSe_{22.5}$ under photo illumintaion. The total time of crystallization shows a decrease with increasing temperature but it is longer for the samples annealed under photo illumination.

Table I

Conductivity-temperature dependence of photo-illuminated $SSe_{22.5}$ samples annealed at different isotherms

Annealing temp., °C	$-\log \sigma\ (\Omega\ \mathrm{cm})^{-1}$		Total change		First stage (ab)		Second stage (cd)	
	Initial	Final	$\Delta \log \sigma$	Δt, min	$\Delta \log \sigma_1$	Δt_1	$\Delta \log \sigma_2$	Δt_2
98	9.69	6.60	3.09	285	One stage process			
108	9.26	6.21	3.05	210	0.45	15	2.56	192
117	9.47	5.55	3.92	175	1.16	14	2.82	149
121	9.55	5.47	4.08	160	1.09	13	2.93	144
126	9.69	5.18	4.51	120	1.27	9	3.26	110
132	9.87	5.01	4.86	100	One stage process			
144	9.80	5.34	4.46	53	One stage process			

Plate 1 is a typical reflection micrograph pattern (X450) taken for $SSe_{22.5}$ thin film isothermally annealed at 100 °C for 2 hrs with 2.13 eV incident photons. This value is greater than the known value of dissociation energy of Se—Se bond, 1.8 eV [14]—1.9 eV [15]. Plate 2 is for an identical $SSe_{22.5}$ film annealed at 100 °C in the dark. The plates show that the growth is faster in the dark and leads to a more ordered crystalline network. The absorbed quanta of light produce, however, an increase in the number of dispersed centres. Also, the difference in the grain size due to illumination is clear in Plates 1 and 2.

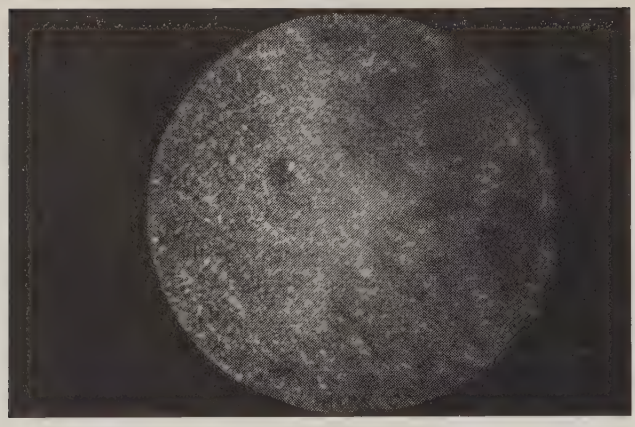

1

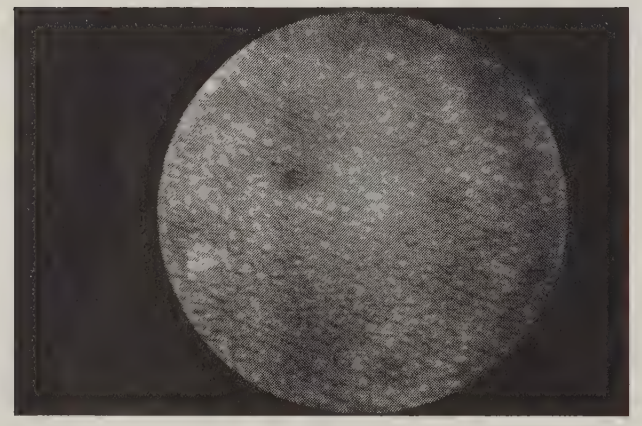

2

Plates 1 and 2: Typical micrograph patterns for Se doped with 4.26 at % S films annealed isothermally at 100 °C for 2 hrs in the presence (Plate 1) and absence (Plate 2) of photo illumination

Changing the energy of the incident photons in the range of 1.91—3.04 eV has no significant effect on the nature and total duration of the transformation process in the studied temperature range.

Crystallization kinetics

To study the kinetics of transformation the experimental data should be expressed in terms of the transformed fraction at different crystallization times. In the present work, $X(t)$ is evaluated for the S-doped Se sample by using the relative increase of the electric conductivity during the growth. This, however, may be realized by considering a power or logarithmic conductivity dependence according to ODELEVSKY [16] and LANDAUER [17], respectively.

For low crystallite volumes, a general power formula is written:

$$\sigma^k = \theta_1 \sigma_1^k + \theta_2 \sigma_2^k,$$

where θ_1 is the fraction left uncrystallized and θ_2 is the corresponding crystallized fraction. For $k = 1$, the conductivity at a time t is

$$\sigma_t = \theta_t \sigma_a + (1 - \theta_t)\sigma_c,$$

i.e.

$$\theta_t(\sigma) = (\sigma_c - \sigma_t)/(\sigma_c - \sigma_a). \tag{1}$$

On the other hand, when $\log \sigma$ is considered to represent the sensitive parameter characterizing the conductivity-content dependence, an empirical popular formula may be written as:

$$\log \sigma = \theta_1 \log \sigma_1 + \theta_2 \log \sigma_2,$$

i.e.

$$\theta_t(\log \sigma) = (\log \sigma_c - \log \sigma_t)/(\log \sigma_c - \log \sigma_a). \tag{2}$$

The subscripts a and c refer to values at the begining and at end of the process. These correspond to points a and d on the curves of Fig. 1.

The extent of crystallization X_t as a function of the annealing time is computed on the basis of Eqs. (1) and (2), and Fig. 2 shows some of these results. The crystallization curves appear to shift toward lower time scales with increasing temperature as one might expect from the decrease in viscosity with increasing temperature.

The crystalllization of organic polymers has been described by the AVRAMI [18] formula

$$X_t = 1 - \exp(-Kt^n), \tag{3}$$

where K is the temperature-dependent rate constant and n is a parameter depending on nucleation and growth mode [19].

To fit AVRAMI's equation, a plot of $\ln[-\ln(1 - X_t)]$ versus $\ln(t)$ must yield a straight line whose slope is n and whose intercept on the ordinate

at $\ln(t) = 0$ is $\ln(K)$. Figs. 3 show just such plots for $SSe_{22.5}$ under the effect of photo illumination. At some temperatures, the plot takes on two distinct slopes during the isothermal crystallization which, therefore, can be described by two different values for both n and K in the rate equation. A change in the exponent n indicates a change in growth mechanism during crystallization, a phenomenon quite well known for polymer systems in which a secondary crystallization occurs after the primary crystallization event [20]. The results for n and K calculated on the basis of the ODELEVSKY approach (Eq. (1)) as well as the LANDAUER approach (Eq. (2)) are summarized in Table II.

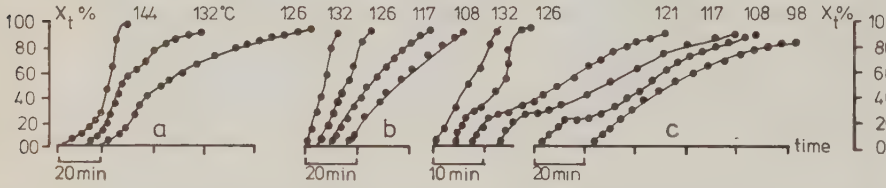

Fig. 2. Crystallinity percent vs annealing time for Se doped with 4.26 at % S derived from d.c. conductivity measurements: (a) and (b) under purely thermal effect, and (c) with photon effect (2.13 eV) on basis of: (a) σ, and (b) and (c) log σ. Here, $X_t = 1 - \theta_t$

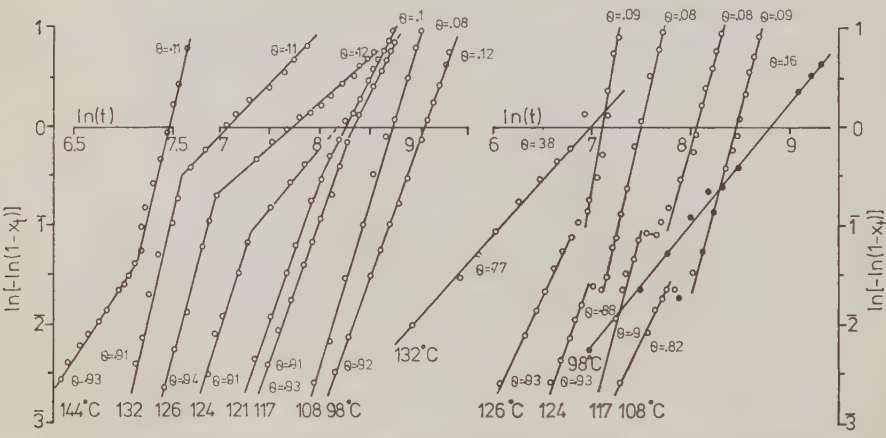

Fig. 3. ln [—ln (1 — X_t)] vs ln (t) plots for crystallization kinetics of photo-illuminated Se doped with 4.26 at % S on the basis of: (a) σ and (b) log σ

The kinetic calculations on the basis of log σ indicate that the crystallization growth under purely thermal effects proceeds by one process as characterized by a single value for n or K. The value of n decreases monotonically with temperature in the range 98—132 °C, while the crystallization rate constant K increases by 30% with temperature from 98 to 132 °C. In Table II, on the other hand, the values of n estimated on basis of σ show that the transforma-

tion clearly consists of two stages at temperatures above 120 °C which account for the presence of secondary crystallization. For the first stage, with θ up to 0.6—0.7, $n_1 > 2$ while for the second $n_2 \simeq 1$ which leads to the conclusion that in this latter stage crystallization is restricted to one-dimensional growth, the driving force is constant, and no new nuclei are formed. The considerably higher values of K_2 than K_1 indicate that the secondary crystallization is a faster process. But, at a relatively high temperature as 144 °C, $n_2 > n_1$ and $K_2 \ll K_1$ which may be ascribed to the limitation of the applicability of the σ-crystallinity correlation (ODELEVSKY approach). While the kinetic calculations on the basis of $\log \sigma$ (LANDAUER approach) indicate that $n_1 = 3.75$ and $n_2 = 1.26$ are consistent with the considered mechanism.

Table II

AVRAMI constants calculated on basis of σ and $\log \sigma$ as conductivity-structure characterization functions for both illuminated and non-illuminated $SSe_{22.5}$

Cryst. temp., °C	Crystallization under photo illumination							
	On basis of σ				On basis of $\log \sigma$			
	n_1	K_1	n_2	K_2	n_1	K_1	n_2	K_2
98	2.76	1.20×10^{-11}	—	—	1.12	7.55×10^{-5}	—	—
108	2.24	1.05×10^{-8}	—	—	1.27	8.30×10^{-5}	1.52	5.25×10^{-6}
117	2.70	1.30×10^{-10}	2.00	4.75×10^{-8}	1.48	1.90×10^{-5}	1.60	2.35×10^{-6}
121	2.75	1.66×10^{-10}	1.9	1.54×10^{-7}	0.92	7.30×10^{-4}	1.68	1.60×10^{-6}
124	3.20	5.05×10^{-11}	1.72	1.10×10^{-6}	0.88	9.60×10^{-4}	1.80	1.30×10^{-6}
126	3.80	1.10×10^{-11}	0.98	1.75×10^{-3}	0.86	1.45×10^{-3}	2.48	2.55×10^{-8}
132	4.20	5.30×10^{-13}	1.04	6.30×10^{-4}	1.24	1.60×10^{-4}	—	—
144	1.56	3.60×10^{-6}	4.10	5.00×10^{-14}	2.64	1.90×10^{-8}	0.94	1.69×10^{-3}

Cryst. temp., °C	Crystallization in the dark							
	On basis of σ				On basis of $\log \sigma$			
	n_1	K_1	n_2	K_2	n_1	K_1	n_2	K_2
98	3.20	1.45×10^{-13}	—	—	1.24	1.65×10^{-5}	—	—
108	2.20	1.05×10^{-8}	—	—	1.15	7.90×10^{-5}	—	—
117	1.50	6.35×10^{-6}	—	—	1.14	1.25×10^{-4}	—	—
121	1.80	4.78×10^{-7}	—	—	1.13	1.70×10^{-4}	—	—
124	2.40	1.50×10^{-8}	1.14	1.25×10^{-4}	1.12	2.10×10^{-4}	—	—
126	2.42	2.20×10^{-8}	1.12	1.65×10^{-4}	1.10	2.70×10^{-4}	—	—
132	2.48	3.50×10^{-8}	1.16	2.35×10^{-4}	1.08	5.28×10^{-4}	—	—
144	2.14	8.30×10^{-8}	6.50	1.55×10^{-21}	3.75	1.00×10^{-11}	1.26	1.66×10^{-4}

Subscripts 1 and 2 refer to the presence of primary and secondary modes.

Evidently, there is correspondence between the present kinetics for $SSe_{22.5}$ computed on the basis of σ and that of CRYSTAL [2] for pure Se computed from densitometric data. Doping of S leads to generating the secondary crystallization at a temperature about 124 °C instead of at 100 °C for Se [2, 21]. The big difference between the rate constant K for $SSe_{22.5}$ and that

of Se identifies the effect of addition of 4.26 at % S in inhibiting the crystallization process of Se.

The photo effect on the kinetics of $SSe_{22.5}$ as obtained on the basis of log σ shows two AVRAMI exponents referring to two growth stages defining the crystallization process in the range 108—126 °C (Fig. 3b). The observed kink between the two kinetic lines lies in the region of pronounced photo effect and corresponds to $\theta \simeq 0.7$. However, these results for n_1 (Table II), refer to one-dimensional nucleation growth which seems to be unrealistic.

Apart from this, AVRAMI's values of n_1 as reflected by σ changes (Fig. 3a), are 2.24 to 4.2 in the range 98—132 °C and those of n_2 fall in the range 1—2 which confirms the expected one-dimensional growth of binding the terminals of the formed individual crystallites as they come close to each other. A secondary crystallization has started at 117 °C which represents a lower temperature than that in dark, 124 °C. Moreover, nucleation of $SSe_{22.5}$ observed in the optical microscope is definitely heterogeneous in the entire temperature range studied. Heterogeneous nucleation has been found in liquid-crystalline transformation for pure Se and S-doped Se samples too [21].

However, the dramatic variation of the kinetic parameter n may be attributed to the complex nature of the crystallization of materials of Se-like structure compared with most polymers and other materials first described by AVRAMI theory.

A more detailed investigation of the effect of light on the process of crystallization is under way; the results will be published in the near future.

REFERENCES

1. B. FITTON and C. H. GRIFFITHS, J. Appl. Physics, **39**, 3663, 1968.
2. R. C. CRYSTAL, J. Polym. Sci., *A*-2, **8**, 1755, 1970.
3. M. C. COUGHLIN and B. WUNDERLICH, Kolloid Z. Z. Polym., **250**, 482, 1972.
4. M. C. COUGHLIN and B. WUNDERLICH, J. Polym. Sci., **11**, 1735, 1973.
5. J. SCHOTTMILLER, M. TABAK, G. LUCOVSKY and A. WARD, J. Non-Cryst. Solids, **4**, 80, 1970.
6. M. K. EL-MOUSLY, J. Neorg. Mat. (USSR), **13**, 801, 1977.
7. M. K. EL-MOUSLY and M. F. KOTKATA, Acta Phys. Hung., **43**, 117, 1977.
8. J. DRESNER and G. B. STRINGFELLOW, J. Phys. Chem. Solids, **29**, 303, 1968.
9. I. A. PARIBOK-ALEXANDROVICH, Soviet Phys.-Solid State, **11**, 1631, 1970.
10. J. FEINLEIB, J. DE-NEUFVILLE, S. C. Moss and S. R. OVSHINSKY, Appl. Phys. Lett., **18**, 254, 1971.
11. A. D. PEARSON and B. G. BAGLEY, Mat. Res. Bull., **6**, 1041, 1971.
12. R. G. BRANDES, F. B. LAMING and A. D. PEARSON, Appl. Optics, **9**, 1712, 1970.
13. K. P. MAMEDOV and Z. D. NURIEVA, Soviet Phys. Cryst., **12**, 605, 1968.
14. T. L. COTTROLL, "The Strength of Chemical Bonds", 2nd Ed., Butterworths, London, 1958, p. 258.
15. L. PAULING, "The Nature of the Chemical Bond", 3rd Ed., Cornell University Press, Ithaca, 1960, p. 85.
16. V. I. ODELEVSKY, J. Technical Physics (USSR), **21**, 673, 1951.
17. R. LANDAUER, J. Appl. Phys., **23**, 7, 77, 1952.
18. M. AVRAMI, J. Chem. Phys., **7**, 1103, 1939; ibid., **8**, 212, 1940; ibid., **9**, 117, 1941.
19. L. MANDELKORN, "Crystallization of Polymers", McGraw-Hill, New York, 1964.
20. F. RYBNIKAR, J. Polym. Sci., 44, 517, 1960.
21. M. K. EL-MOUSLY, M. F. KOTKATA and S. A. SALAM, J. Physics C, **11**, 1077, 1978.

Acta Physica Academiae Scientiarum Hungaricae, Tomus 46 (1), pp. 27—30 (1979)

DEBYE-WALLER FACTORS OF PLATINUM AND LEAD

By

K. N. Mehrotra and J. P. Dixit

DEPARTMENT OF PHYSICS, D.A.V. COLLEGE, KANPUR 208001, INDIA

(Received in revised form 10. XII. 1978)

The Debye—Waller factor temperature parameters at different temperatures for platinum and lead have been calculated by using a modified Sharma and Joshi model. The calculations were carried out according to previous results [1]. Comparison of theoretical results with available experimental data, as presented in the vibration spectrum dependent Debye—Waller factor temperature parameter (Y) versus temperature diagrams, reveals reasonably satisfactory agreement.

I. Introduction

In a previous paper [1] we have used the modified Sharma and Joshi model for the theoretical investigation of the temperature dependence of Debye—Waller factors of five FCC metals: copper, silver, gold, nickel and aluminium. The purpose of the present paper is to report on similar studies carried out with FCC platinum and lead. Theory and the method of the calculation were described in [1], to which the interested reader is referred for details. In this paper, similarly to paragraph IV in [1], we only wish to present and discuss results obtained with Pt and Pb. The various constants needed in the calculations are listed in Table I.

Table I

Constants and the parameters used in the calculation

Metal	Atomic mass in a.m.u.	Elastic constants (10^{11} dyn/cm^2)			Ref.	Temp.* (K)	Lattice parameter (Å)	Phonon frequencies (THz)			Ref.
		C_{11}	C_{12}	C_{44}				$\nu_L(100)$	$\nu_T(100)$	$\nu_L\left(\frac{1}{2}\frac{1}{2}\frac{1}{2}\right)$	
Platinum	195.09	34.67	25.07	7.65	a	300	3.924	5.789	3.750	5.650	c
Lead	207.19	4.953	4.229	1.49	b	300	4.9504	1.910	0.955	2.212	d

* Temperature at which the elastic constants are measured.

a. R. E. Macfarlane, J. A. Rayne and C. K. Jones, Phys. Lett., **18,** 91, 1965.
b. D. L. Waldorf and G. A. Alers, J. Appl. Phys., **33,** 3266, 1962.
c. R. Ohrlich and W. Drexel, Inelastic Scattering of Neutrons in Solids and Liquids, Vol. 1, International Atomic Energy Agency, Vienna, 1968 p. 203.
d. R. Stedman, L. Almqvist, G. Nilsson and G. Raunio, Phys. Rev., **162,** 545, 1967.

II. Results and discussion

1. *Platinum*

Alexopoulos et al [2] have studied the temperature dependence of the Debye characteristic temperature for platinum by measuring the temperature variation of the integrated X-ray intensity of the (331), (420), (422) and (531) reflections from flat powder samples in the range of 100—700 °K. The values of the Debye—Waller factor temperature parameter Y obtained from these authors together with our calculated results are shown in Fig. 1 with the reference temperature $T_0 = 293$ °K. The agreement of the calculated Y values with experiment is satisfactory.

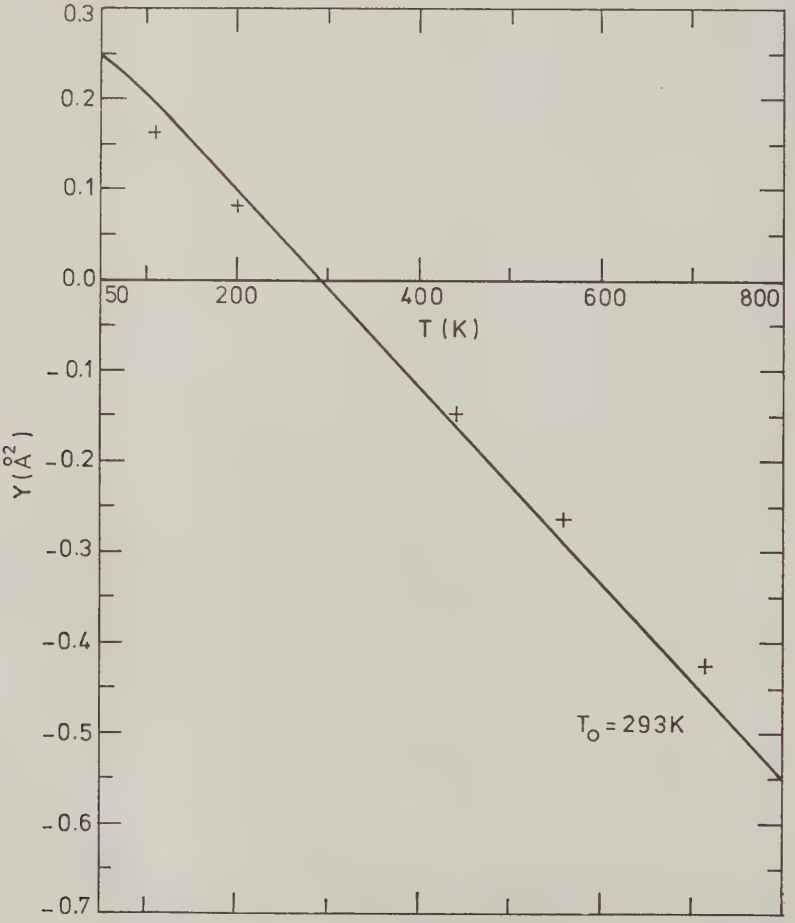

Fig. 1. Variation of Y for platinum. Solid line shows the present calculation. Experimental points: + Alexopoulos et al.

. *Lead*

The temperature dependence of the intensity of the X-ray reflections om lead has been studied by CARTZ [3], CHIPMAN and PASKIN [4], IOTHERSOLE and OWEN [5], CHIPMAN [6], and ALEXOPOULOS et al [2]. CARTZ as obtained the temperature variation of the Debye characteristic temperature or lead by measuring the intensity of the diffuse scattering of X-rays from ngle crystals at temperatures ranging from 150 to 600 °K. He also made orrection for Compton scattering. CHIPMAN nad PASKIN carried out measure- ents on lead powder at room and liquid nitrogen temperatures. MOTHERSOLE nd OWEN investigated in the temperature range 293—577 °K on fine grade

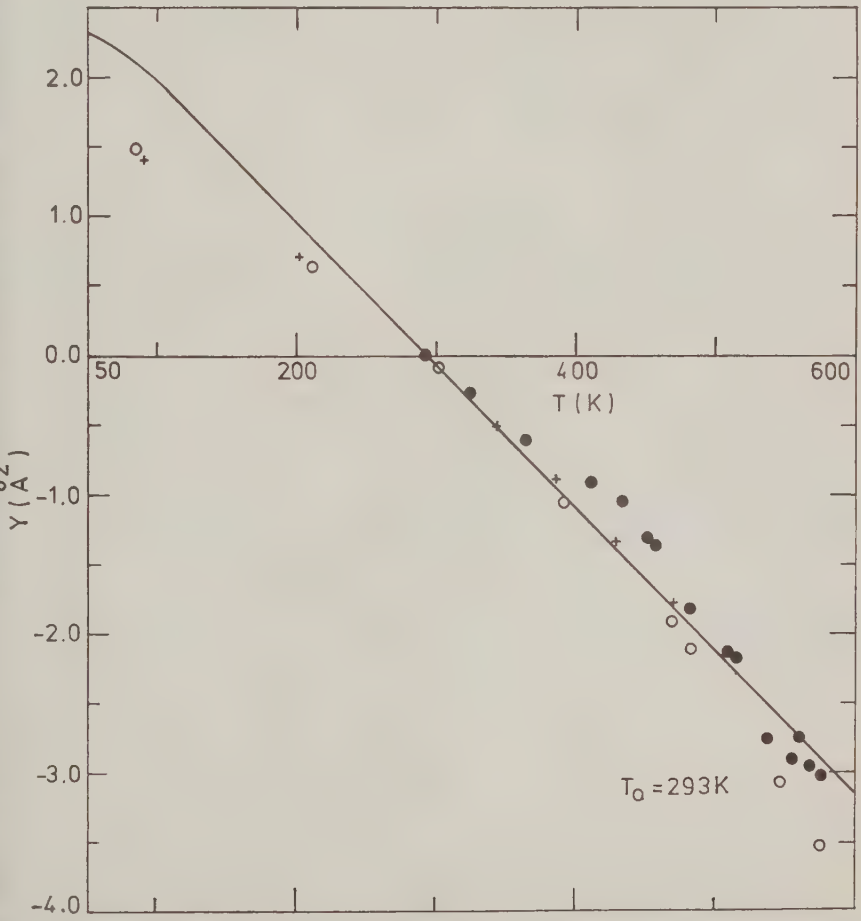

Fig. 2. Variation of Y for lead. Experimental points: ○ CHIPMAN; ● MOTHERSOLE and OWEN; + ALEXOPOULOS et al.

powder specimens. The Table summarising the results of these authors contains the values of Y at selected temperatures. CHIPMAN obtained the temperature variation of the Debye characteristic temperature by measuring the integrated intensity of a high angle X-ray diffraction peak between 85—576 °K correcting also for the thermal diffuse scattering (TDS). ALEXOPOULOS et al used flat powder samples in the temperature range of 100—500 °K for the reflections (331), (420), (422), (511)—(533), (531), (600)—(442). For the present comparison the data of MOTHERSOLE and OWEN, CHIPMAN, and ALEXOPOULOS et al were selected. The results are presented in Fig. 2 with $T_0 = 293$ °K. The theoretical results agree reasonably well with the experimental values.

The actual discrepancies between theory and experiment could be attributed to various causes discussed already in [1]. Nevertheless one may conclude that our attempt to explain the observed temperature variation of the Debye—Waller factors for platinum and lead on the basis of the modified Sharma and Joshi model appears to be successful.

Acknowledgement

One of the authors (J.P.D.) wishes to thank the University Grants Commission, New Delhi, for financial assistance.

REFERENCES

1. J. P. DIXIT and K. N. MEHROTRA, Acta Phys. Hung., **42**, 127, 1977.
2. K. ALEXOPOULOS, J. BOSKOVITS, S. MOURIKIS and M. ROILOS, Acta Cryst., **19**, 349, 1965.
3. L. CARTZ, Proc. Phys. Soc., **B68**, 951, 1955.
4. D. R. CHIPMAN and A. PASKIN, J. Appl. Phys., **30**, 1992, 1959.
5. N. MOTHERSOLE and E. A. OWEN, Brit. J. Appl. Phys., **16**, 1113, 1965.
6. D. R. CHIPMAN, J. Appl. Phys., **31**, 2012, 1960.

Acta Physica Academiae Scientiarum Hungaricae, Tomus 46 (1), pp. 31—37 (1979)

NON-LINEAR HYDROMAGNETIC WAVES IN TWO-ELECTRON TEMPERATURE PLASMA

By

M. L. Mittal and D. Govinda Thirtha

DEPARTMENT OF MATHEMATICS, INDIAN INSTITUTE OF TECHNOLOGY, BOMBAY 400 076, INDIA

(Received 12. XII. 1978)

The non-linear hydromagnetic waves for two-electron temperature plasma are shown to be governed by a Korteweg—de Vries—Burgers equation. Collisional effects have also been taken into account. Due to the magnetic field the amplitude of the solitary wave decreases while the width of the soliton and the speed of the shock wave increase.

1. Introduction

Following the work of Jones et al [1] on two-electron temperature plasma, there is a wide range of interest in the study of such plasmas due to its application in many physical problems. Goswami and Buti [2] considered the ion acoustic solitary waves in such a plasma with one of the species of the electrons as cold and obtained the condition for the existence of solitary waves. Shukla and Tagare [3] included the effects of collisions by considering fluid equations with ion viscosity and ion thermal conductivity. They have shown that shock-like structures evolve when the temperature difference between the two components of electrons is fairly large.

In the present note the effects of uniform magnetic field on non-linear hydromagnetic waves in two-electron temperature plasma are investigated. The magnetic field is considered in the $x-z$ plane making an angle θ with the x-axis. Using the perturbation scheme given by Davidson [4], a Korteweg—de Vries—Burgers equation governing the hydromagnetic waves is derived. Both collisional and collisonless plasmas are considered and solitary wave and shock wave solutions are obtained.

2. Analysis

Following Shukla and Tagare [3], the governing wave equations in the presence of a magnetic field can be written as

$$\frac{\partial n_i}{\partial t} + \frac{\partial}{\partial x}(n_i u_{ix}) = 0, \tag{1}$$

$$\frac{\partial u_{ix}}{\partial t} + u_{ix}\frac{\partial u_{ix}}{\partial x} + \frac{1}{n_i}\frac{\partial}{\partial x}(n_i T_i) = E_x + R_i(u_{iy}B_z - u_{iz}B_y) + \frac{4}{3}\eta_i \frac{\partial^2 u_{ix}}{\partial x^2}, \quad (2)$$

$$\frac{\partial u_{iy}}{\partial t} + u_{ix}\frac{\partial u_{iy}}{\partial x} = E_y + R_i(u_{iz}B_x - u_{ix}B_z) + \frac{4}{3}\eta_i \frac{\partial^2 u_{iy}}{\partial x^2}, \quad (3)$$

$$\frac{\partial u_{iz}}{\partial t} + u_{ix}\frac{\partial u_{iz}}{\partial x} = E_z + R_i(u_{ix}B_y - u_{iy}B_x) + \frac{4}{3}\eta_i \frac{\partial^2 u_{iz}}{\partial x^2}, \quad (4)$$

$$\frac{3}{2}\left(\frac{\partial T_i}{\partial t} + u_{ix}\frac{\partial T_i}{\partial x}\right) + T_i \frac{\partial u_{ix}}{\partial x}$$

$$= k_i \frac{\partial^2 T_i}{\partial x^2} - \frac{1}{A^2 R_i}\left(\frac{\partial B_z}{\partial x}E_y - \frac{\partial B_y}{\partial x}E_z\right) + \frac{3}{4}\eta_i\left(\frac{\partial u_{ix}}{\partial x}\right)^2, \quad (5)$$

$$\frac{T_{ef}}{T_{el}} n_{el} E_x + \frac{\partial n_{el}}{\partial x} = 0, \quad (6)$$

$$\frac{T_{ef}}{T_{eh}} n_{eh} E_x + \frac{\partial n_{eh}}{\partial x} = 0, \quad (7)$$

$$-M\frac{\partial E_x}{\partial x} = n_{eh} + n_{el} - n_i, \quad (8)$$

$$A^2 R_i n_i u_{iy} = -\frac{\partial B_z}{\partial x}, \quad (9)$$

$$A^2 R_i n_i u_{iz} = \frac{\partial B_y}{\partial x}, \quad (10)$$

$$\frac{\partial E_z}{\partial x} = R_i \frac{\partial B_y}{\partial t}, \quad (11)$$

$$\frac{\partial E_y}{\partial x} = -R_i \frac{\partial B_z}{\partial z}. \quad (12)$$

In Eqs, (1) to (12), the ion density n_i, ion flow velocity u_i, ion temperature T_i, electric field E, magnetic field B and variables x and t are the non-dimensionalised with respect to N_0, C_{sf}, T_{ef}, T_{ef}/eL, B_0, L and L/C_{sf} respectively, where

$$C_{sf} = \left[\frac{T_{ef}}{m_i}\right]^{1/2}, \quad T_{ef} = \frac{T_{eh}T_{el}}{N_{eh}T_{el} + N_{el}T_{eh}},$$

$$R_i = \frac{\omega_i}{\omega_0}, \quad A = \frac{C_{sf}}{V_A}, \quad M = \left[\frac{\lambda_{Df}}{L}\right]^2.$$

N_0 is total electron density, ω_0 characteristic frequency, λ_{Df} Debye length, L characteristic scale length. Subscript i is used for ions and the subscripts

eh and *el* are used for high temperature and low temperature components of isothermal electrons.

Introducing the stretched variables $\xi = \varepsilon^{1/2}(x - V_P t)$ and $\tau = \varepsilon^{3/2} t$ ($\varepsilon^{1/2}$ is a small parameter proportional to the wave number and V_P is the non-dimensional phase velocity of the wave) and assuming E_x, E_z, B_y, u_{iy}, η_i and k_i to be of the order of $\varepsilon^{1/2}$ all the dependent variables are expanded as series of ε around the uniform state as follows:

$$g = g_0 + \sum_{j=1}^{\infty} \varepsilon^j g^{(j)}, \tag{13}$$

where g stands for dependent variables and g_0 represents the equilibrium state so that

$$g_0 = \begin{cases} 1,\ N_{e1},\ N_{eh} & \text{for the densities of ions, low and high-temperature electrons, respectively;} \\ 0 & \text{for all components of velocity and electric field;} \\ \cos\theta,\ 0,\ \sin\theta & \text{for the three components of the magnetic field;} \\ T_{i0} & \text{for the ion temperature.} \end{cases}$$

Substituting Eq. (13) in Eqs. (1) to (12) and equating the coefficients of ε, one has

$$V_p = \left[1 + \frac{5}{3} T_{i0} + \frac{\sin^2\theta}{A^2}\right]^{1/2}. \tag{14}$$

The phase velocity V_p in Eq. (14) is the same as the velocity of propagation of hydromagnetic waves which one can obtain for the same plasma system in the linear approximation.

Equating the coefficients of ε^2 in Eqs. (1) to (12) and eliminating the second order dependent variables, a Korteweg—de Vries—Burgers equation is obtained for $n_i^{(1)}$ as given below:

$$\frac{\partial n_1^{(i)}}{\partial \tau} + \frac{1}{2V_P}\left[(3 - \Delta) + \frac{40 T_{i0}}{9} + \frac{2\sin^2\theta}{A^2}\right] n_i^{(1)} \frac{\partial n_i^{(1)}}{\partial \xi} + \frac{1}{2V_P}\left[M + \frac{\sin^2\theta}{A^4 R_i^2}\left(1 - \frac{\cos^2\theta}{A^2 V_P^2}\right)\right] \frac{\partial^3 n_i^{(1)}}{\partial \xi^3} - 2\left[\frac{\eta_0}{3} + \frac{k_0 T_{i0} V_P^{-2}}{9}\right] \frac{\partial^2 n_i^{(1)}}{\partial \xi^2} = 0. \tag{15}$$

Here $\Delta = [N_{eh} T_{eh}^{-2} + N_{el} T_{e1}^{-2}] T_{ef}^2$, $\eta_i = \varepsilon^{1/2} \eta_0$, $k_i = \varepsilon^{1/2} k_0$.

In Eq. (15), the coefficient of third term describes the effect of dispersion.

For further discussion, Eq. (15) is written as

$$P_1^{-1}\frac{\partial f}{\partial \tau}+f\frac{\partial f}{\partial \varepsilon}+\beta_1\frac{\partial^3 f}{\partial \varepsilon^3}-\mu_1\frac{\partial^2 f}{\partial \varepsilon^2}=0 \tag{16}$$

which resembles the Korteweg—de Vries—Burgers equation obtained by Shukla and Tagare [3]. But here

$$P_1=\left[(3-\Delta)+\frac{40T_{i0}}{9}+\frac{2\sin^2\theta}{A^2}\right]\Big/2V_p;$$

$$\beta_1=\frac{M+\dfrac{\sin^2\theta}{A^4R_i^2}\left(1-\dfrac{\cos^2\theta}{A^2V_p{}^2}\right)}{(3-\Delta)+\dfrac{40T_{i0}}{9}+\dfrac{2\sin^2\theta}{A^2}}$$

and

$$\mu_1=\frac{2}{P_1}\left(\frac{\eta_0}{3}+\frac{k_0\,T_{i0}\,V_p^{-2}}{9}\right).$$

For stationary solution. Eq. (16) yields

$$\beta_1\frac{d^2f}{d\chi^2}-\mu_1\frac{df}{d\chi}+\frac{1}{2}f^2-\left(\frac{U}{P_1}\right)f=0, \tag{17}$$

where $\chi=\xi-U\tau$ and $U=v_0/C_{sf}$.

The solitary wave solution of Eq. (17) in the limit $\mu_1/\beta_1\to 0$ will be

$$f=3U\left(\frac{1}{P_1}\right)\operatorname{sech}^2\left[\left(\frac{U}{4P_1\beta_1}\right)^{1/2}(\xi-U\tau)\right]. \tag{18}$$

In the finite limit of μ_1/β_1, Eq. (17) describes a shock wave [5] and the effective potential well is given by

$$V(f)=\frac{f^3}{6}-\frac{U}{2P_1}f^2. \tag{19}$$

The speed of the shock wave in the rest frame is

$$v_0=C_{sf}\left(1+\frac{P_1\bar{f}}{2}\right), \tag{20}$$

where $\bar{f}=f(-\infty)-f(\infty)$ and $f(\infty)=0$.

Following the method of KARPMAN [5], one can show that Eq. (17) has a monotonic shock wave solution when $\mu_1 > \mu_{1cr}$ and an oscillatory shock wave solution when $\mu_1 < \mu_{1cr}$ where

$$\mu_{1cr} = (2\beta_1 \bar{f})^{1/2}. \tag{21}$$

If $\mu_1 \ll \mu_{1cr}$, then the stationary solution is given by

$$f = \bar{f} + \text{const.} \exp\left(\frac{\mu_1}{2\beta_1}\chi\right) \cos\left[\left(\frac{\bar{f}}{2\beta_1}\right)^{1/2}\chi\right]. \tag{22}$$

3. Numerical calculations and conclusions

Eq. (18) shows that due to the presence of magnetic field and the ion temperature, the range of Δ for which the solitary wave exists is increased. The solitary wave exists for $\Delta < 3 + \frac{5T_{i0}}{3} + \frac{2\sin^2\theta}{A^2}$. But an additional condition must be satisfied, i.e.

$$\frac{\lambda_D^2}{L^2} = M \geq \frac{\sin^2\theta}{A^4 R_i^2}\left(1 - \frac{\cos^2\theta}{A^2 V_P^2}\right). \tag{23}$$

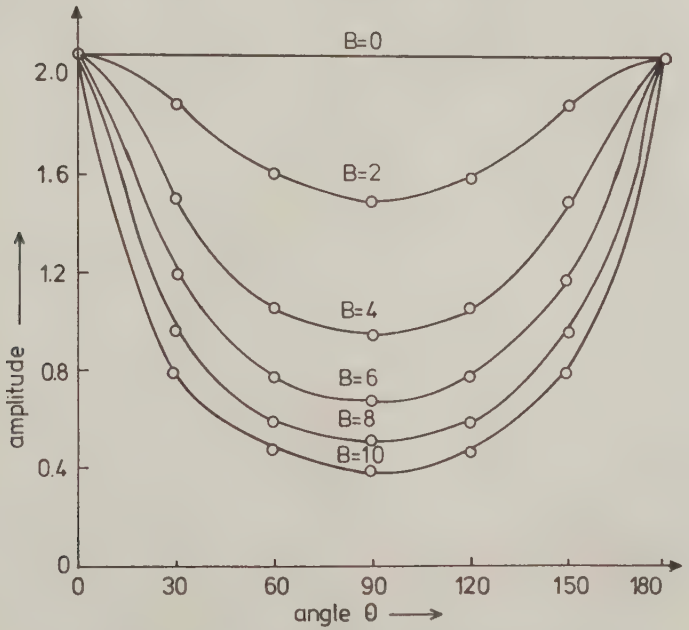

Fig. 1. Variation of the amplitude of the solitary wave w.r. to angle θ

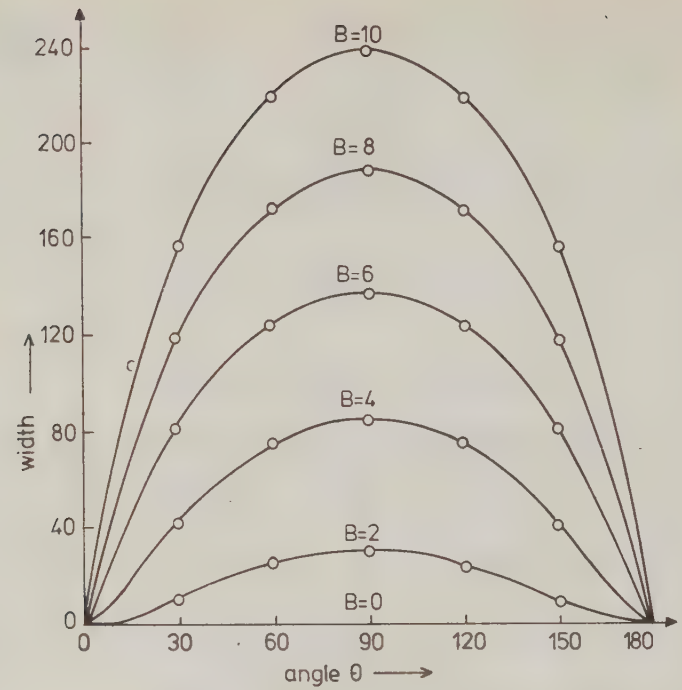

Fig. 2. Variation of width of the solitary wave w.r. to angle θ

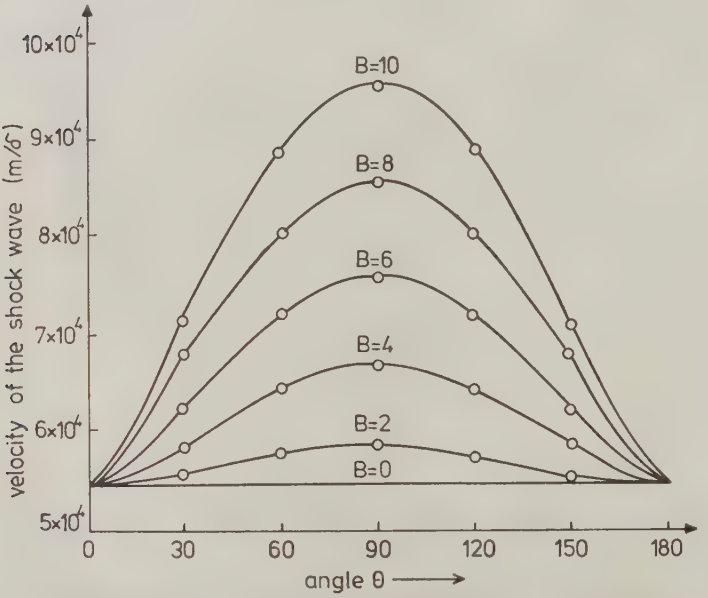

Fig. 3. Variation of the velocity of the shock wave w.r. to angle θ

compared to the obvious condition $M \geq 0$ in the absence of applied magnetic field. Some sample calculations have been made to show the effect of magnetic field explicitly on the amplitude and width of the solitons and the speed of the shock wave for a plasma with the following parameters:

$$T_i = 10^4\ ^\circ\mathrm{K}, \qquad N_0 = 10^{24}\ m^{-3}, \qquad L = 0.1\ \mathrm{m},$$
$$T_{e1} = 2 \times 10^5\ ^\circ\mathrm{K}, \qquad N_{e1} = N_{eh} = 0.5 \times 10^{24}\ \mathrm{m}^{-3}, \qquad U = f = 1,$$
$$T_{eh} = 3 \times 10^5\ ^\circ\mathrm{K}, \qquad B = 2 \text{ to } 10 \text{ Tesla}, \qquad \eta_0 = k_0 = 1.$$

The amplitude and the width of the solitary wave are plotted in Figs. 1 and 2 for various values of the magnitude and direction of the magnetic field. The amplitude of the solitary wave decreases whereas its width increases as the magnitude of the magnetic field increases. The effect of the magnetic field is strongest for perpendicular propagation where it tends to flatten the soliton. Fig. 3 gives the speed of the shock wave and it is seen that it increases with the magnetic field.

REFERENCES

1. W. D. Jones, A Lee, S. M. Cleman and H. J. Doucet, Phys. Rev. Lett., **35**, 1349, 1975.
2. B. N. Goswami and B. Buti, Phys. Lett., **57A**, 149, 1976.
3. P. K. Shukla and S. G. Tagare, Phys. Lett., **59A**, 38, 1976.
4. R. C. Davidson, Methods in Nonlinear Plasma Theory, Academic Press, New York, Chap. 2, 1972.
5. V. I. Karpman, Nonlinear Waves in Dispersive Media, Pergamon Press, Oxford, 1975.

Acta Physica Academiae Scientiarum Hungaricae, Tomus 46 (1), pp. 39—43 (1979)

SIMILARITY SOLUTIONS FOR PLANE RELATIVISTIC FLOW IN A HOMOGENEOUS MEDIUM

By

G. Deb Ray

DEPARTMENT OF MATHEMATICS, ST. XAVIER'S COLLEGE, CALCUTTA-16, INDIA

(Received 27. XII. 1978)

Similarity solutions in closed forms for propagation of plane shock waves in a relativistic gas of uniform number density are obtained. The shock moves with constant speed.

Introduction

Similarity solutions for one-dimensional flow of a relativistic fluid headed by a shock front in a cold gas are studied by Eltgroth [2], by assuming the velocity of the fluid as the similarity variable.

In the present paper similarity solutions in closed forms are obtained when the plane shock front moves through a homogeneous medium of uniform nucleon number density.

The origin of the (x, t) inertial co-ordinate frame is taken at a plane where an initial disturbance is given.

We find that such a flow for the similarity parameter $\xi = x^a t^b$, a and b being suitable constants, exists only when the shock moves with a constant velocity. The solutions given in this paper are applicable only to a medium of uniform pressure or a cold gas.

Equations of motion and boundary conditions

$$\frac{\partial}{\partial x}\left\{\frac{p + \beta^2 E}{1 - \beta^2}\right\} + \frac{\partial}{\partial\, ct}\left\{\frac{\beta(p + E)}{1 - \beta^2}\right\} = 0, \tag{1}$$

$$\frac{\partial}{\partial x}\left\{\frac{\beta(p + E)}{1 - \beta^2}\right\} + \frac{\partial}{\partial ct}\left\{\frac{E + \beta^2 p}{1 - \beta^2}\right\} = 0, \tag{2}$$

$$\frac{\partial}{\partial x}\left\{\frac{n\beta}{\sqrt{1 - \beta^2}}\right\} + \frac{\partial}{\partial ct}\left\{\frac{n}{\sqrt{1 - \beta^2}}\right\} = 0, \tag{3}$$

where p is the pressure and E the proper energy density, both measured in the rest frame of the fluid; $c\beta$ is the fluid velocity in the (x, t) inertial frame, c being the speed of light and n is the nucleon number density.

The shock conditions are

$$\left[\frac{p+\beta^2 E}{1-\beta^2}\right]=\frac{dX}{dct}\left[\frac{\beta(p+E)}{1-\beta^2}\right], \tag{4}$$

$$\left[\frac{\beta(p+E)}{1-\beta^2}\right]=\frac{dX}{dct}\left[\frac{E+\beta^2 p}{1-\beta^2}\right], \tag{5}$$

$$\left[\frac{n\beta}{(1-\beta^2)^{1/2}}\right]=\frac{dX}{dct}\left[\frac{n}{(1-\beta^2)^{1/2}}\right]. \tag{6}$$

Here [ ] signifies the discontinuity sign and $\mathrm{d}X/\mathrm{d}t$ is the velocity of the shock, X being the distance of the shock plane from the origin.

The nucleon density of the pre-shock stage is given by

$$n_0 = \text{constant}. \tag{7}$$

Solutions of the equations

We next introduce the following similarity transformations as done by COURANT and FRIEDRICHS [1] for non-relativistic motions of gases:

$$c\beta = \frac{x}{t}\,U(\xi),$$

$$p = x^{k+2}\,t^{\lambda-2}\,P(\xi),$$

$$E = x^{k+2}\,t^{\lambda-2}\,Z(\xi),$$

$$n = x^k\,t^\lambda\,\Omega(\xi),$$

where

$$\xi = x^a t^b.$$

Here λ, k, a and b are constants to be determined from the problem.

By their direct substitutions in Eqs. (1)—(3) and boundary conditions (4)—(6), we find that these forms are compatible only when we choose $a/b = -1$ and $\lambda + k = 0$. Without any loss we take $a = 1$ and $b = -1$, $\lambda = 0$ and $k = 0$.

For our subsequent work we choose the similarity parameter in dimensionless form as

$$\eta = \frac{x}{ct}. \tag{8}$$

At the shock front $\eta = \eta_0$ and is taken as constant. So,

$$\eta_0 = \frac{X}{ct} = \frac{V}{c}, \tag{9}$$

V being the constant velocity of the shock front.

The boundary conditions at the shock front may be re-written as

$$\frac{p_1}{p_0} = \frac{\beta_1 \eta_0 N + 1}{1 - \beta_1 \eta_0}, \tag{10}$$

$$\frac{E_1}{E_0} = \frac{\eta_0 N + \beta_1}{N(\eta_0 - \beta_1)}, \tag{11}$$

$$\frac{n_1}{n_0} = \eta_0 \frac{(1 - \beta_1^2)^{1/2}}{\eta_0 - \beta_1}, \tag{12}$$

where $N = E_0/p_0$and the subscripts 1 and 0 stand respectively for quantities just behind the shock and just in front of it.

We find that unlike its non-relativistic analogue, there are two characteristic parameters, instead of one, namely, $\eta_0 = V/c$ and N, depending on the equation of state of matter in its pre-shock condition.

In the region behind the shock plane we take the equation of state,

$$p = \frac{1}{3} E. \tag{13}$$

Eqs. (1)—(3) are now transformed as

$$\frac{d}{d\eta}\left[\frac{E(1/3 + \beta^2)}{1 - \beta^2}\right] = \eta \frac{d}{d\eta}\left[\frac{4/3\, \beta E}{1 - \beta^2}\right], \tag{14}$$

$$\frac{d}{d\eta}\left[\frac{4/3\, \beta E}{1 - \beta^2}\right] = \eta \frac{d}{d\eta}\left[\frac{E(1 + \beta^2/3)}{1 - \beta^2}\right], \tag{15}$$

$$\frac{d}{d\eta}\left[\frac{n\beta}{\sqrt{1 - \beta^2}}\right] = \eta \frac{d}{d\eta}\left[\frac{n}{\sqrt{1 - \beta^2}}\right]. \tag{16}$$

Combining (1) and (2) we also find as Eltgroth [2]

$$\frac{1}{E}\frac{dE}{d\eta} = \pm \frac{4}{\sqrt{3}} \cdot \frac{1}{(1 - \beta^2)} \frac{d\beta}{d\eta}. \tag{17}$$

Eqs. (1) and (2) are next re-arranged as

$$\frac{1}{E}\frac{dE}{d\eta} = \frac{d\beta}{d\eta} \cdot \frac{4}{(1 - \beta^2)} \cdot \frac{(\beta^2 \eta + \eta - 2\beta)}{(1 + 3\beta^2 - 4\beta\eta)} \tag{18}$$

and

$$\frac{1}{E}\frac{dE}{d\eta} = \frac{d\beta}{d\eta} \cdot \frac{4}{(1-\beta^2)} \cdot \frac{(2\beta\eta - 1 - \beta^2)}{(4\beta - 3\eta - \eta\beta^2)}, \tag{19}$$

Comparing (18) and (19) with (17) when $d\beta/d\eta \neq 0$, we get,

$$\frac{\beta^2\eta + \eta - 2\beta}{1 + 3\beta^2 - 4\beta\eta} = \frac{2\beta\eta - 1 - \beta^2}{4\beta - 3\eta - \eta\beta^2} = l, \tag{20}$$

where

$$l = \frac{1}{\sqrt{3}} \text{ or } -\frac{1}{\sqrt{3}}.$$

The trial $l = \frac{1}{\sqrt{3}}$ yields as a solution

$$\beta = \frac{\sqrt{3}\,\eta - 1}{\sqrt{3} - \eta} \tag{21}$$

and $l = -\frac{1}{\sqrt{3}}$, represents the solution

$$\beta = \frac{\sqrt{3}\,\eta + 1}{\sqrt{3} + \eta}. \tag{22}$$

Case I

We next investigate the existence of solutions for the case $N = 3$, which is appropriate for an ultra-relativistic initial state.

For the choice $n_0 = \text{const.}$ (Eq. (7)), we easily find from the shock conditions that in this case both E_0 and p_0 are constants.

Eqs. (10) and (11) now give

$$\beta_1 = \frac{3\eta_0^2 - 1}{2\eta_0}, \quad 0 < \eta_0 < 1 \text{ and } |\beta_1| \leq 1. \tag{23}$$

Besides, the solution (21) is consistent with (23) only when $\eta_0 = \frac{1}{\sqrt{3}}$ and $\eta_0 = 1$. Both these values of η_0 are not tenable, as $\eta_0 = \frac{1}{\sqrt{3}}$ in this case implies the shock speed as equivalent to the speed of sound and $\eta_0 = 1$, the shock speed attaining the photonic speed. The solution (22) is also inconsistent with the requirement (23).

So, for the medium considered here, we should take the other alternative in Eqs. (18) and (19), namely, $d\beta/d\eta = 0$

Hence,

$$\beta = \beta_1 \tag{24}$$

$$E = E_1 \tag{25}$$

and

$$n = n_1, \tag{26}$$

which are all constants.

Case II

Next we seek solutions for the other possibility $p_0 = 0$, appropriate for a cold gas. The modified shock conditions yield

$$\beta_1 = \frac{2\eta_0 \pm \sqrt{4\eta_0^2 - 3}}{3}. \tag{27}$$

Solution (21) is consistent with (27), only when $\eta_0 = \frac{\sqrt{3}}{2}$ and so $\beta_1 = \frac{1}{\sqrt{3}}$. Besides, it is found that solution (22) is unfavourable and extraneous.

For the value of β as given by (21), and from (18) and (16), respectively, we find that

$$\log \frac{E}{E_1} = \frac{2}{\sqrt{3}}\left[\log \frac{1+\eta}{1-\eta} + 2 \log (2 - \sqrt{3})\right], \tag{28}$$

$$\log \frac{n}{n_1} = \frac{\sqrt{3}}{2}\left[\log \frac{1+\eta}{1-\eta} + 2 \log (2 - \sqrt{3})\right]. \tag{29}$$

In this case if the gas is pushed instantaneously and thereby set into motion, there is a possible backflow as clearly indicated by our solutions. As $\eta \to -1$, both the energy density and number density tend to zero, thereby showing that a portion of matter moves backward and the edge of vacuum is at $\eta = -1$. At this boundary we find that the relativistic material moves with the speed of light into the vacuous region.

REFERENCES

1. R. Courant and K. O. Friedrichs, Supersonic Flow and Shock Waves, Inter Sc., New York, 1948.
2. P. G. Eltgroth, Phys. Fluids, **14**, 2631, 1971.

Acta Physica Academiae Scientiarum Hungaricae, Tomus 46 (1), pp. 45—51 (1979)

EXCITATION PROCESSES IN A HOLLOW-CATHODE He—Zn DISCHARGE*

By

E. Lőrincz, P. Richter and I. Péczeli

DEPARTMENT OF ATOMIC PHYSICS, TECHNICAL UNIVERSITY, 1521 BUDAPEST

(Received 30. I. 1979)

Spectroscopic and electronic parameters of a hollow-cathode discharge in the mixture of He and Zn vapour were measured. The excitation processes important for the operation of metal vapour lasers are discussed under different conditions of the discharge.

1. Introduction

Research has been carried out for a long time on noble gas — metal vapour lasers. CW operation and excitation mechanisms of a He—Zn ion laser as a function of different parameters (current and pressure dependence of the output power) are described in [1]. Possible excitations of Zn II levels were examined using flowing afterglow technique in [2, 3] and [4].

In the present experiments the excitation processes of the He—Zn system were examined in a hollow cathode discharge tube by measuring spectroscopic (spontaneous line intensities) and electronic (discharge current and voltage) parameters. The results give information on the processes in the hollow cathode discharge and the excitation of the 4912 Å Zn II laser line.

2. Experimental details

The geometry of the hollow cathode discharge tube used in the experiments is shown in Fig. 1. The required Zn concentration in the tube was maintained by two ovens at equal temperatures. The discharge tube was evacuated by a small vacuum system that consisted of a mechanical and an oil diffusion pump and could be filled by high purity ($>$99.999%) He gas. The tube was excited by half-wave rectified current. The light from the discharge was imaged to the entrance slit of a Zeiss PGS-2 2 m spectrograph, used as a monochromator. The line intensities selected were measured by a photo-

* The present work has been carried out under a contract with the Central Research Institute for Physics of the Hungarian Academy of Sciences.

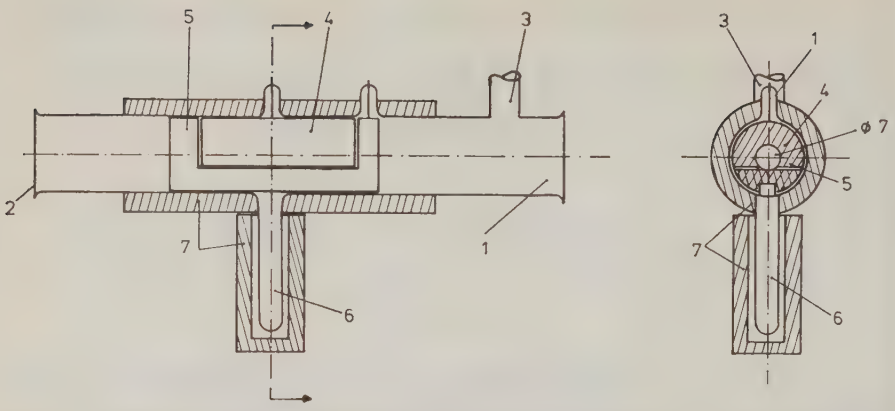

Fig. 1. The hollow cathode discharge tube 1. pyrex tube, 2. end window, 3. connection to the vacuum system, 4. cathode, 5. anode, 6. Zn metal, 7. ovens

multiplier IP28. The output of the multiplier or the discharge voltage was measured with an oscilloscope as a function of discharge current using the horizontal input of the oscilloscope for the latter.

3. Experimental results

Variation of the discharge voltage with the pressure is shown in Fig. 2 at $T = 20$ °C for three values of current. In order to be able to interpret these curves the line intensity of He II at 4685 Å was measured under the same conditions (Fig. 3). Above 6 torr a close correlation can be observed between the two sets of curves.

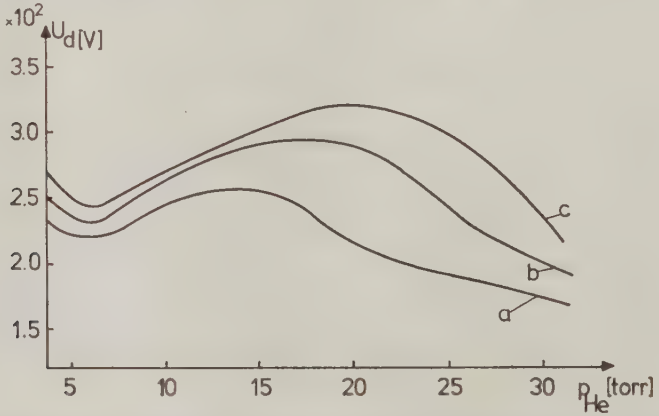

Fig. 2. The variation of discharge voltage with He pressure for different currents a. $I = 126$ mA; b. $I = 252$ mA; c. $I = 378$ mA

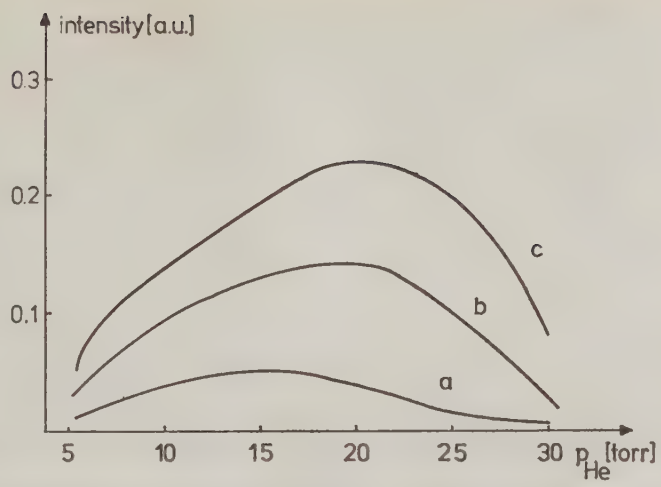

Fig. 3. The intensity of the 4685 Å He II line as a function of the pressure at $T = 20$ °C
a. $I = 126$ mA; b. $I = 252$ mA; c. $I = 378$ mA

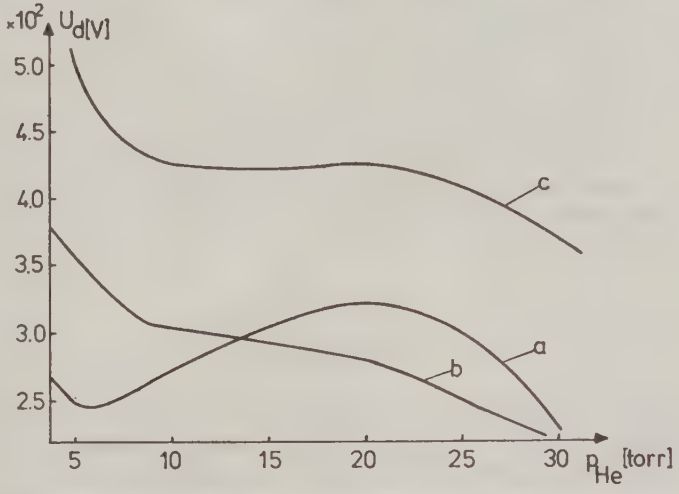

Fig. 4. The dependence of the discharge voltage on He pressure at constant current ($I = 378$ mA) for different oven temperatures (Zn concentration)
a. $T = 20$ °C; b. $T = 440$ °C; c. $T = 500$ °C

Next the voltage dependence on the pressure was measured for different Zn concentrations that were set by keeping the temperatures of the two ovens at determined and equal values. Fig. 4. shows that a low Zn concentration (the melting point of Zn is 419.6 °C) changes the original curve significantly and increasing Zn concentration raises the discharge voltage. Fig. 5 shows the

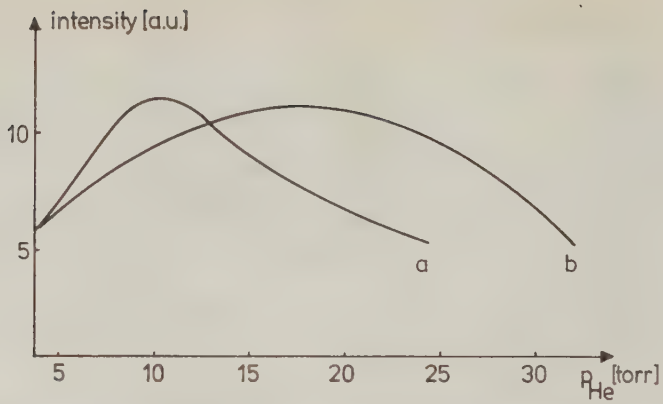

Fig. 5. The intensity of the 4912 Å Zn line as a function of He pressure at constant current ($I = 378$ mA) at different oven temperatures i.e. Zn concentrations a. $T = 440$ °C, b. $T = 500$ °C

variation of the spontaneous light intensity of the 4912 Å Zn II laser line with He pressure for two different Zn concentrations. At 440 °C there is a sharp He pressure dependence while at a higher temperature the curve broadens.

In Fig. 6 (a, b, c) the discharge voltage (a) spontaneous line intensity of Zn II at 4912 Å (b), and spontaneous line intensity of Zn I at 4810 Å (c) are plotted as a function of temperature i.e. Zn concentration at constant He pressure. It can be seen that while the discharge voltage and the intensity of the atomic line increases monotonously with rising Zn concentration the ion line saturates around 500 °C.

4. Discussion

The pressure dependence of the intensity of the 4685 Å spectral line of He II (Fig. 3) justifies the fact that the increase of discharge voltage with pressure above the minimum at 6 torr (Fig. 2) is caused by the increase of He ionization rate. The ionization potential of He is very large (about 25 eV) that means significant electron energy is lost in the course of an elementary ionization process, thus in order to maintain the constant current larger voltage is required. The drop of the discharge voltage at high pressure is probably in connection with the fact that the current is partly displaced from the hollow into the gap between the anode and the cathode in rate this pressure region. It was not possible to measure He ionization rate in the presence of Zn because the upper level for the 4685 Å He II line is of very high energy (about 51 eV) and therefore this level is not populated in the presence of a

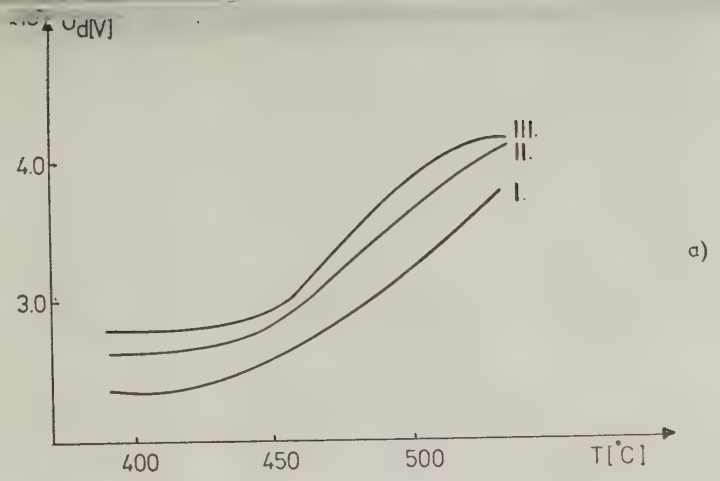

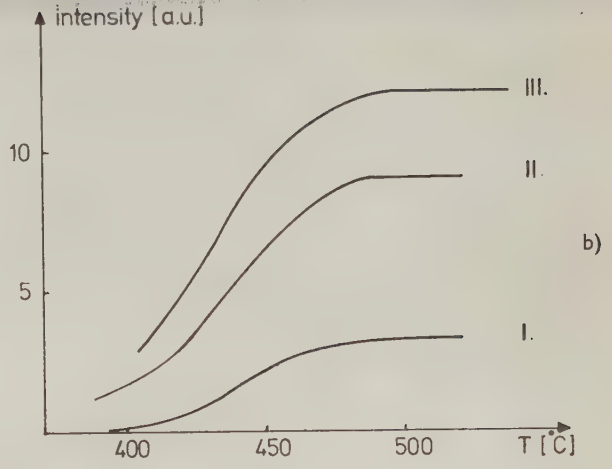

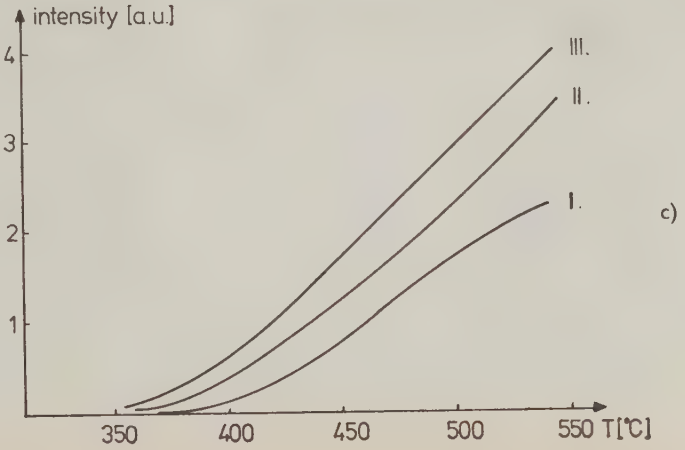

Fig. 6. The discharge voltage (6a), the intensity of the 4912 Å Zn II line (6b), and the intensity of the 4810 Å Zn I line (6c) as a function of oven temperatures, i.e. Zn concentration. He pressure = 10 torr, current I: 126 mA, II: 252 mA, III: 378 mA

component with low ionization potential. No transition in the visible starts from a lower energy level of He II. Still the He ion concentration could be deduced indirectly from Figs. 4 and 5. At a low concentration of Zn ($T = 440$ °C) the intensity of the 4912 Å Zn II line is maximum at about 10 torr of He and shows a strong dependence on He pressure. This observation supports the assumption that in the selective excitation of the $4f^2F$ Zn II level the charge transfer (Duffendach) collisions

$$He^+ + Zn \rightarrow He + Zn^{+*}$$

play an important role. The detailed mechanism of the excitation is described in [3]. This means that the ionization of He is still significant at this temperature. At $T = 500$ °C the He pressure dependent selective excitation of the 4912 Å Zn II line washes out and at the same time a significant increase in discharge voltage can be observed (Figs. 5 and 6/a). In order to interpret this effect one has to consider the properties of the hollow cathode discharge. Neglecting the effect of electrons produced by photoeffect the current density is [5]

$$j = j_c^+(1 + \gamma) = eN_c^+v_c^+(1 + \gamma),$$

where j_c^+ is the ion current density on the cathode, γ stands for the secondary electron emission, N_c^+ and v_c^+ are the ion density and ion mobility, respectively.

The increase of discharge voltage may be caused by the fact that due to their lower ionization potential the Zn^+ ions take over the main role in the ion current gradually. In order to reach the cathode to produce secondary electron emissions that is necessary for the stable discharge, the Zn^+ ions can achieve the energy necessary only at a higher voltage due to their larger masses. Therefore in this region most probably direct electron collisions play the most important role in the excitation of the 4912 Å Zn II line because of the decreased He^+ ion concentration. In this way the selective excitation to the upper laser level is spoiled, that may be the reason why the optimum Zn concentration in He — Zn lasers can be reached at a temperature much below 500 °C [1, 6]. Unfortunately no direct measurement could be carried out concerning the population of the lower level because there is no transition in the visible range originating from it.

The increase in Zn concentration, as has been pointed out above, leads to a rise of the discharge voltage (Fig. 6/a). Comparing Figs. 6a and 6c it turns out that while the Zn concentration increases uniformly the voltage starts to rise significantly only around 450 °C. This shows that under this temperature the He^+ dominates in the ion current while Zn^+ takes over above it. The spontaneous intensity of the 4912 Å Zn II laser line increases in the

temperature range 400—450 °C (range of selective excitation) more than above it and is saturated around 500 °C. The constant current and pressure limits the ionization in spite of the increasing Zn concentration.

5. Conclusion

It was shown that in the He—Zn hollow cathode discharge variation of He and Zn concentrations leads to changes in the discharge parameters through changing the ionization processes in the discharge. These have important effects on the excitation of the 4912 Å Zn II laser transition, namely at low Zn concentration the selective excitation to the upper level of this line dominate through resonant charge transfer collisions with He^+, while at higher Zn concentration direct electron excitation takes over and the selectivity disappears.

Further measurements will be carried out in the case when the Zn is introduced in the form of a volatile molecule to the same discharge. In this case the sufficient Zn concentration can be reached at a lower temperature and at the same time the presence of the electronegative component may cause changes in the discharge.

Acknowledgements

Thanks are due to Prof. I. Kovács for his help and support and to Drs L. Csillag, M. Jánossy and K. Rózsa for valuable discussions.

REFERENCES

1. J. A. Piper and P. Gill, J. Phys. D8, 127, 1975.
2. A. R. Turner-Smith, J. M. Green and C. E. Webb, J. Phys., B6, 114, 1973.
3. J. M. Green, G. J. Collins and C. E. Webb, J. Phys., B6, 1545, 1973.
4. G. J. Collins, J. Appl. Phys., 44, 4633, 1973.
5. G. Francis in Encyclopedia of Physics, ed. Flügge, Vol XXII. Springer, Berlin—Göttingen, Heidelberg, 1956, p. 108.
6. J. A. Piper and C. E. Webb, J. Phys., D6, 400, 1973.

RECENSIONES

Inelastic Electron Tunneling Spectroscopy

Proceedings of the International Conference and Symposium on Electron Tunneling, University of Missouri—Columbia, USA, May 25—27, 1977. Springer Verlag, Berlin—Heidelberg—New York, 1978.

During the last decades several new material-testing methods have appeared and became generally accepted. A greater part of them is concerned with the investigation of solid surfaces. Let us mention the different electron and ion-irradiating methods (EMP, IMXA), secondary ion mass-spectrometry (SIMS) or the varieties of charged particles activation analysis with nuclear accelerators.

These methods include a separate but substantial group, formed by the different types of electron spectroscopies, by the help of which the spectra of electrons produced by different methods from the surface of solids are investigated, producing qualitative or quantitative or trace- and structure-analytical information. In this respect X-ray and ultra-violet induced photo-electron spectroscopy (XPS alias ESCA and UPS), Auger electron spectroscopy (AES) as well as ion-induced electron spectroscopy (INS) or characteristic energy-loss electron spectroscopy (ELS) should be mentioned.

In spite of its name inelastic electron tunneling spectroscopy (IETS) does not belong to the latter group in the strict sense. Under certain circumstances electrons may penetrate the insulating layer between two metal surfaces (mostly aluminium oxide on Al-surface with Pb evaporated on it) as the result of a quantummechanical tunneling effect. The probability of this penetration depends on the atoms and molecules present at the transition surface and their vibration states, respectively. These appear in the form of a regular spectrum if the second derivative of the current-voltage characteristic of the junction has been taken into consideration. It should be noted here that such investigations are carried out at the temperature of liquid He (4.2 °K) and with modulation techniques. Molecules to be observed e.g. cyclic compounds and materials interesting from the biological point of view should be deposited on the surface of the Al-oxide, in some way. Electron tunneling spectroscopy gives information similar to Raman- and infrared spectroscopy, we may say that it makes them complete.

The book which appeared in one of the Springer series (Series in Solid State Sciences) contains the lectures of an international scientific meeting the aim of which was not only to present and discuss recent scientific results in connection with the method, but also to present the method itself to the wide community of representatives of different fields of application. Thus the book is extremely useful and suitable also for beginners in this field.

The first chapter is devoted to the treatment of the method, the second one to the fields of application, while the third deals with theoretical aspects. Separate chapters are devoted to the description of up-to-date applications, as well as to molecular adsorption on non-metallic surfaces and finally to the application of the so-called elastic tunneling effect.

It is doubtless that IETS seems to possess unique features (e.g. in sensitivity) and to have several possible fields of applications in surface chemistry, biochemistry as well as in the investigation of greasing and adhesion phenomena etc., that is in every field, where the adsorption of complex molecules on metallic oxides have an important role.

Nowadays, however, we may talk about the wide-range possibilities of the method rather than about its justified applications. This fact is pointed out in the contributions by two surface-research scientists and a biologist (Chapter IV, Discussions and Comments). From this point of view tunneling spectroscopy has not achieved yet the maturity so far achieved by electron spectroscopy in the strict sense (XPS, UPS or APS).

D. Berényi

A Perspective of Physics

Volume 2. Selections from 1977 Comments on Modern Physics. Introduced and put into perspective by Sir Rudolf Peierls.

Gordon and Breach Science Publishers, London—New York—Paris, 1978.

It is good to see the second volume of this highly promising series that gives a very useful insight into different fields of physics both by the ingeniously written introduction by Sir Rudolf Peierls and by his careful selection of papers from Comments on Modern Physics by distinguished researchers of their fields.

Rereading the introduction of Vol. 1 one can clearly see the trends in the different branches of physics from the comparison with Vol. 2. The selected papers give a short and clear view of the field they represent. In this way a coherent picture is received by the reader from a very wide subject.

At the same time the individual papers represent most recent research thus giving a useful reference for the specialists as well.

The main chapters are: Nuclear and Particle Physics, Solid State Physics, Astrophysics, Atomic and Molecular Physics, Plasma Physics and Controlled Fusion.

P. Richter

E. W. Williams and R. Hall:

Luminescence and the Light Emitting Diode

International Series on Science of the Solid State. General Editor: B. R. Pamplin, Pergamon Press, Oxford, New York, Toronto, Sidney, Paris, Frankfurt 1978.

This book offers the readers a comprehensive survey of the physics and technology of the light emitting devices (LED's) and p-n junction lasers. The book begins with a good introduction to crystal structures and growth, and the optical and electrical properties of LED materials.

In Chapter 3 the authors summarize the different single crystal growth methods used generally in LED production. A short discussion of the fabrication of the devices together with a useful data collection regarding diffusion processes are included in Chapter 4. A simplified theory of the radiative and nonradiative recombination processes, the luminescent efficiency and the solid-state lasers made from LED materials are discussed in Chapters 5 and 6.

The most important characterization measurement methods such as the photoluminescence, the cathodluminescence, capacity measurements, diode emission evaluation techniques (flux, intensity and colour measurements) are described in detail in Chapters 7 and 8 offering a good physical insight into the light emitting processes in the most important LED materials GaAs, GaP and GaAsP.

In Chapter 9 a survey of light emitting diodes is given together with the discussion of the relationship between aspects of LED design and the electro-optical characteristics. The remainder of the Chapter reviews the progress achieved in producing LED's from different materials.

The book ends with the application aspects of LED products, which are divided into three main groups: (a) LED indicator lamps, (b) LED displays, (c) optically coupled devices.

Although this book is written for post-graduate students, it seems to be useful to a much wider range of readers who would like to know more about LED and the materials from which it is made.

T. Görög

Gánti, Tibor:

A THEORY OF BIOCHEMICAL SUPER-SYSTEMS. Its application to problems of natural and artificial biogenesis

The *chemoton theory* represents a conceptionally new approach to the deduction of the simplest physical—chemical, macromolecular super-systems satisfying those criteria of life which have been reformulated by the author almost axiomatically, in a more exact presentation than commonly known from the literature. The prospects of the further development of the theory are promising, because the principles of the chemoton model are simple and clear, making the deduction of many basic biological phenomena possible already in its present form, and offering a feasible explanation for the origin of living systems from which the outlines of the strategy for the artificial synthesis of living systems also emerge.

In English — Approx. 80 pages — 17×25 cm — ISBN 963 05 1719 1 — Cloth

AKADÉMIAI KIADÓ, Budapest
Publishing House of the Hungarian Academy of Sciences

Vértes, Attila — Korecz, László — Burger, Kálmán:

MÖSSBAUER SPECTROSCOPY

The introductory part of the book summarizes the physical fundamentals of Mössbauer spectroscopy, the purport of information obtainable from the parameters characterizing the spectrum, and the technique of measurement. The other chapters review the results obtained by applying Mössbauer spectroscopy in the chemistry of solutions, coordination chemistry, quantum chemistry, metallurgy and biochemistry. The material contained in these chapters enables researchers to collect information in their respective branches of science, in addition, they are able to gain insight into the possibilities of the useful applications of the Mössbauer effects for solving problems in their special field.

In English — Approx. 380 pages — Cloth — ISBN 963 05 1670 5

AKADÉMIAI KIADÓ, Budapest **ELSEVIER SCIENTIFIC PUBLISHING COMPANY, Amsterdam**

A new volume in the successful series

ABSORPTION SPECTRA IN THE INFRARED REGION

Ed. by L. LÁNG

Volume 5

This is the fifth volume of the series which presents the infrared spectra of selected organic compounds over the range 400—4000 cm^{-1}, together with full details of sample and experimental conditions. The empirical formula, molecular weight and melting point of each substance is also given. The choice of the spectra has been made by a panel of experienced spectroscopists, who have given primary considerations to covering compounds which have been isolated or synthetized recently. More familiar materials have also been included, generally because the spectra presented for them are more detailed than those of other published sources, or because they refer to different experimental conditions.

The volumes of ABSORPTION SPECTRA IN THE INFRARED REGION provide a valuable source of reference which complements and extends existing sources. Organic chemists and biochemists in academic and industrial laboratories, particularly in the petrochemicals and pharmaceuticals industries, will find this series an easily accessible source of clearly presented infrared spectra of an interesting range of compounds.

In English — Approx. 320 pages — Spectra of 300 compounds — 21×29 cm — ISBN 963 05 1768 X — Cloth

AKADÉMIAI KIADÓ, Budapest

E. KRIEGER PUBLISHING CO. INC., Huntington

Printed in Hungary

kiadásért felel az Akadémiai Kiadó igazgatója. Műszaki szerkesztő: Botyánszky Pál
kézirat a kiadóba érkezett: 1979. II. 1. — A kézirat nyomdába érkezett: 1979. II. 6. — Terjedelem : 5,25 (A/5) ív, 25 ábra

79.6777 Akadémiai Nyomda, Budapest — Felelős vezető: Bernát György

NOTES TO CONTRIBUTORS

I. PAPERS will be considered for publication in Acta Physica Hungarica, only if they have not previously been published or submitted for publication elsewhere. They may be written in English, French, German or Russian.

Papers should be submitted to

Prof. I. Kovács, Editor
Department of Atomic Physics, Technical University
1521 Budapest, Budafoki út 8, Hungary

Papers may be either articles with abstracts or short communications. Both should be as concise as possible, articles in general not exceeding 25 typed pages, short communications 8 typed pages.

II. MANUSCRIPTS

1. Papers should be submitted in five copies.

2. The text of papers must be of high stylistic standard, requiring minor corrections only.

3. Manuscripts should be typed in double spacing on good quality paper, with generous margins.

4. The name of the author(s) and of the institutes where the work was carried out should appear on the first page of the manuscript.

5. Particular care should be taken with mathematical expressions. The following should be clearly distinguished, e.g. by underlining in different colours: special founts (italics, script, bold type, Greek, Gothic, etc.); capital and small letters; subscripts and superscripts, e.g. x_2, x^3; small l and 1; zero and capital O; in expressions written by hand: e and l, n and u, v and v, etc.

6. References should be numbered serially and listed at the end of the paper in the following form: J. Ise and W. D. Fretter, Phys. Rev., *76*, 933, 1949.

For books, please give the initials and family name of the author(s), title, name of publisher, place and year of publication, e.g.: J. C. Slater, Quantum Theory of Atomic Structures, I. McGraw-Hill Book Company, Inc., New York, 1960.

References should be given in the text in the following forms: Heisenberg [5] or [5].

7. Captions to illustrations should be listed on a separate sheet, not inserted in the text.

III. ILLUSTRATIONS AND TABLES

1. Each paper should be accompanied by five sets of illustrations, one of which must be ready for the blockmaker. The other sets attached to the copies of the manuscript may be rough drawings in pencil or photocopies.

2. Illustrations must not be inserted in the text.

3. All illustrations should be identified in blue pencil by the author's name, abbreviated title of the paper and figure number.

4. Tables should be typed on separate pages and have captions describing their content. Clear wording of column heads is advisable. Tables should be numbered in Roman numerals (I, II, III, etc.).

IV. MANUSCRIPTS not in conformity with the above Notes will immediately be returned to authors for revision. The date of receipt to be shown on the paper will in such cases be that of the receipt of the revised manuscript.

Reviews of the Hungarian Academy of Sciences are obtainable at the following addresses:

AUSTRALIA
C.B.D. LIBRARY AND SUBSCRIPTION SERVICE, Box 4886, G.P.O., *Sydney N.S.W. 2001*
COSMOS BOOKSHOP, 145 Acland Street, *St. Kilda (Melbourne), Victoria 3182*

AUSTRIA
GLOBUS, Höchstädtplatz 3, *1200 Wien XX*

BELGIUM
OFFICE INTERNATIONAL DE LIBRAIRIE, 30 Avenue Marnix, *1050 Bruxelles*
LIBRAIRIE DU MONDE ENTIER, 162 Rue du Midi, *1000 Bruxelles*

BULGARIA
HEMUS, Bulvar Ruszki 6, *Sofia*

CANADA
PANNONIA BOOKS, P.O. Box 1017, Postal Station "B", *Toronto, Ontario M5T 2T8*

CHINA
CNPICOR, Periodical Department, P.O. Box 50, *Peking*

CZECHOSLOVAKIA
MAD'ARSKÁ KULTURA, Národní třida 22, *115 66 Praha*
PNS DOVOZ TISKU, Vinohradská 46, *Praha 2*
PNS DOVOZ TLAČE, *Bratislava 2*

DENMARK
EJNAR MUNKSGAARD, Norregade 6, *1165 Copenhagen*

FINLAND
AKATEEMINEN KIRJAKAUPPA, P.O. Box 128, *SF-00101 Helsinki 10*

FRANCE
EUROPERIODIQUES S. A., 31 Avenue de Versailles, *78170 La Celle St.-Cloud*
LIBRAIRIE LAVOISIER, 11 rue Lavoisier, *75008 Paris*
OFFICE INTERNATIONAL DE DOCUMENTATION ET LIBRAIRIE, 48 rue Gay-Lussac, *75240 Paris Cedex 05*

GERMAN DEMOCRATIC REPUBLIC
HAUS DER UNGARISCHEN KULTUR, Karl-Liebknecht-Strasse 9, *DDR-102 Berlin*
DEUTSCHE POST ZEITUNGSVERTRIEBSAMT, Strasse der Pariser Kommüne 3—4, *DDR-104 Berlin*

GERMAN FEDERAL REPUBLIC
KUNST UND WISSEN ERICH BIEBER, Postfach 46, *7000 Stuttgart 1*

GREAT BRITAIN
BLACKWELL'S PERIODICALS DIVISION, Hythe Bridge Street, *Oxford OX1 2ET*
BUMPUS, HALDANE AND MAXWELL LTD., Cowper Works, *Olney*, Bucks *MK46 4BN*
COLLET'S HOLDINGS LTD., Denington Estate, *Wellingborough*, Northants *NN8 2QT*
W.M. DAWSON AND SONS LTD., Cannon House *Folkestone, Kent CT19 5EE*
H. K. LEWIS AND CO., 136 Gower Street, *London WC1E 6BS*

GREECE
KOSTARAKIS BROTHERS, International Booksellers, 2 Hippokratous Street, *Athens-143*

HOLLAND
MEULENHOFF-BRUNA B.V., Beulingstraat 2, *Amsterdam*
MARTINUS NIJHOFF B.V., Lange Voorhout 9—11, *Den Haag*
SWETS SUBSCRIPTION SERVICE, 347b Heereweg, *Lisse*

INDIA
ALLIED PUBLISHING PRIVATE LTD., 13/14 Asaf Ali Road, *New Delhi 110001*
150 B-6 Mount Road, *Madras 600002*
INTERNATIONAL BOOK HOUSE PVT. LTD., Madame Cama Road, *Bombay 400039*
THE STATE TRADING CORPORATION OF INDIA LTS., Books Import Division, Chandralok, 36 Janpath, *New Delhi 110001*

ITALY
EUGENIO CARLUCCI, P.O. Box 252, *70100 Bari*
INTERSCIENTIA, Via Mazzé 28, *10149 Torino*
LIBRERIA COMMISSIONARIA SANSONI, Via Lamarmora 45, *50121 Firenze*
SANTO VANASIA, Via M. Macchi 58, *20124 Milano*
D. E. A., Via Lima 28, *00198 Roma*

JAPAN
KINOKUNIYA BOOK-STORE CO. LTD., 17-7 Shinjuku-ku 3 chome, Shinjuku-ku, *Tokyo 160-91*
MARUZEN COMPANY LTD., Book Department, P.O. Box 5050 Tokyo International, *Tokyo 100-31*
NAUKA LTD. IMPORT DEPARTMENT, 2-30-19 Minami Ikebukuro, Toshima-ku, *Tokyo 171*

KOREA
CHULPANMUL, *Phenjan*

NORWAY
TANUM-CAMMERMEYER, Karl Johansgatan 41—43, *1000 Oslo*

POLAND
WĘGIERSKI INSTYTUT KULTURY, Marszałkowska 80, *Warszawa*
CKP I W ul. Towarowa 28 *00-958 Warsaw*

ROUMANIA
D. E. P., *București*
ROMLIBRI, Str. Biserica Amzei 7, *București*

SOVIET UNION
SOJUZPETCHATJ — IMPORT, *Moscow*
and the post offices in each town
MEZHDUNARODNAYA KNIGA, *Moscow G-200*

SPAIN
DIAZ DE SANTOS, Lagasca 95, *Madrid 6*

SWEDEN
ALMQVIST AND WIKSELL, Gamla Brogatan 26, *101 20 Stockholm*
GUMPERTS UNIVERSITETSBOKHANDEL AB, Box 346, *401 25 Göteborg 1*

SWITZERLAND
KARGER LIBRI AG, Petersgraben 31, *4011 Basel*

USA
EBSCO SUBSCRIPTION SERVICES, P.O. Box 1943, *Birmingham, Alabama 35201*
F. W. FAXON COMPANY, INC., 15 Southwest Park, *Westwood, Mass. 02090*
THE MOORE-COTTRELL SUBSCRIPTION AGENCIES, *North Cohocton, N. Y. 14868*
READ-MORE PUBLICATIONS, INC., 140 Cedar Street, *New York, N. Y. 10006*
STECHERT-MACMILLAN, INC., 7250 Westfield Avenue, *Pennsauken* N. J. 08110

VIETNAM
YXUNHASABA, 32, Hai Ba Trung, *Hanoi*

YUGOSLAVIA
JUGOSLAVENSKA KNJIGA, Terazije 27, *Beograd*
FORUM, Vojvode Mišića 1, *21000 Novi Sad*

Index: 26.025
Acta Phys. Hung. Tom. 46. No. 1. Budapest, 30. VII. 1979 HU-ISSN 0001-6705